The Influence of Climate on Ozone Risk for Vegetation

Jenny Klingberg

Ph.D. thesis

Department of Plant and Environmental Sciences
University of Gothenburg

Faculty of Science

UNIVERSITY OF GOTHENBURG

The Influence of Climate on Ozone Risk for Vegetation

Jenny Klingberg

2011

UNIVERSITY OF GOTHENBURG
Department of Plant and Environmental Sciences
Faculty of Science

Doctoral Thesis in Applied Environmental Science
Department of Plant and Environmental Sciences, University of Gothenburg

ISBN 978-91-85529-47-6
Available at: http://hdl.handle.net/2077/25120
© Jenny Klingberg, 2011
Printed in Sweden by Intellecta Infolog AB, Göteborg

Front page photo: Mobile monitoring station at Nidingen, 2007

Abstract

Ground-level ozone (O_3) is a harmful air pollutant causing reduced crop yield and quality, reduced forest growth and negative effects on human health in large parts of the world. O_3 is generally seen as a regional scale air pollution problem, but O_3 concentration ($[O_3]$) variation on a smaller geographical scale can be considerable. Knowledge of the size of this local scale variation and the underlying causes is important in environmental monitoring and assessments of O_3 exposure. The local scale variation in $[O_3]$ in Sweden was investigated and described in relation to local climate and site characteristics such as altitude, topography, vicinity to the coast and local NO emissions based on measurements of $[O_3]$ and meteorology with a mobile monitoring station. In addition, $[O_3]$ and $[NO_2]$ were measured with passive diffusion samplers and $[O_3]$ data from permanent monitoring stations were analysed. The strength of nocturnal temperature inversions was found to be crucial in determining the differences in average $[O_3]$ and diurnal $[O_3]$ range (DOR) at rural sites in southern Sweden. Inland low sites experienced stronger nocturnal temperature inversions, lower average $[O_3]$ and larger DOR compared to inland high and coastal sites. In addition, the underlying surface (important for the deposition rate), advection of O_3-rich marine air and local NO emissions also influence the local scale variation of $[O_3]$. The negative effects of O_3 on vegetation are more closely related to the plant uptake of O_3 through the stomata than to the $[O_3]$ in the ambient air. Environmental factors such as humidity, temperature and light, influence the degree of stomatal opening and thus the stomatal O_3 flux into the leaf interior. The flux-based POD_Y-index (phytotoxic O_3 dose above a flux threshold Y) was used to assess the O_3 risk for vegetation. It allows modification of O_3 uptake by climatic conditions to be incorporated in O_3 risk assessment for vegetation. A large part of the local scale variation in $[O_3]$ in southern Sweden occurs during night-time. At night the stomatal O_3 uptake by vegetation is low and the risk of O_3 damage is therefore not greatly influenced. Thus, plant stomatal O_3 uptake and O_3 risk for vegetation are less influenced by the site position in the landscape than 24-hour average $[O_3]$. At the coastal sites the $[O_3]$ were higher also during daytime, which implies an increased risk of negative effects of O_3 on vegetation compared to inland sites. The influence of potential future climate change on the flux-based risk of negative effects of O_3 on vegetation in Europe was investigated with modelled future $[O_3]$ from the chemistry transport model MATCH and meteorology from the regional climate model RCA3. The future plant O_3 uptake and risk of O_3 damage to vegetation was predicted to remain unchanged or decrease in Europe, despite substantially increased modelled $[O_3]$ in Central and Southern Europe. The expected reduction in stomatal conductance with rising atmospheric $[CO_2]$ is of large importance for this result. However, the magnitude of the CO_2 effect is uncertain, especially for trees. If the CO_2 effect will turn out to be small, future climate change has the potential to dramatically increase the flux-based O_3 risk for vegetation in Northern and Central Europe.

Keywords: local climate, topography, nocturnal temperature inversions, ozone spring peak, passive diffusion sampler, AOT40, stomatal ozone flux, stomatal conductance, phytotoxic ozone dose, EMEP, MATCH, RCA3, climate change

The Influence of Climate on Ozone Risk for Vegetation

Jenny Klingberg
(née Sundberg)
2011

This thesis is based on the following papers, which in the text are referred to by their respective Roman numerals.

I. **Sundberg J**, Karlsson P E, Schenk L and Pleijel H (2006) *Variation in ozone concentration in relation to local climate in south-west Sweden*, Water Air and Soil Pollution 173:339-354

II. **Klingberg J**, Björkman M, Pihl Karlsson G and Pleijel H (2009) *Observations of ground-level ozone and NO_2 in northernmost Sweden, including the Scandian Mountain Range*, Ambio 38:448-451

III. **Klingberg J**, Karlsson P E, Pihl Karlsson G, Hu Y, Chen D and Pleijel H *Variation in ozone exposure in the landscape of southern Sweden with consideration of topography and coastal climate*, submitted

IV. Piikki K, **Klingberg J**, Pihl Karlsson G, Karlsson P E and Pleijel H (2009) *Estimates of AOT ozone indices from time-integrated ozone data and hourly air temperature measurements in southwest Sweden*, Environmental Pollution 157:3051-3058

V. **Klingberg J**, Danielsson H, Simpson D and Pleijel H (2008) *Comparison of modelled and measured ozone concentrations and meteorology for a site in south-west Sweden: Implications for ozone uptake calculations*, Environmental Pollution 155:99-111

VI. **Klingberg J**, Engardt M, Uddling J, Karlsson P E and Pleijel H (2011) *Ozone risk for vegetation in the future climate of Europe based on stomatal ozone uptake calculations*, Tellus 63A:174-187

The papers are appended in the end of the thesis and are reproduced with the kind permission from the respective journals.

Scientific publications, co-authored by Jenny Klingberg (née Sundberg), which are not included in this thesis:

- Grundström M, Linderholm H, **Klingberg J** and Pleijel H (2011) *Urban NO_2 and NO pollution in relation to the North Atlantic Oscillation NAO*, Atmospheric Environment 45:883-888

- Pleijel H, **Klingberg J** and Bäck E (2009) *Characteristics of NO_2 pollution in the City of Gothenburg, south-west Sweden - relation to NO_x and O_3 levels, photochemistry and monitoring location*, Water Air and Soil Pollution Focus 9:15-25

- Karlsson P E, Tang L, **Sundberg J**, Chen D, Lindskog A and Pleijel H (2007) *Increasing risk for negative ozone impacts on vegetation in northern Sweden*, Environmental Pollution 150:96-106

- Hageback J, **Sundberg J**, Ostwald M, Chen D, Yun X and Knutsson P (2005), *Climate variability and land-use change in Danangou watershed, China – Examples of small-scale farmers' adaptation*, Climatic Change 72:189-212

Table of contents

Abbreviations

A	Amplitude
A_n	Net photosynthetic rate
$AF_{st}Y$	Accumulated stomatal flux of O_3 above a flux threshold of Y, currently denoted POD_Y.
AOTX	Concentration accumulated over a threshold concentration of X ppb (ppm h)
C	Hourly O_3 concentration
CLRTAP	Convention on Long Range Transboundary Air Pollution
CR	Cooling rate
CTM	Chemistry transport model
DOR	Diurnal O_3 concentration range
DTR	Diurnal air temperature range
EMEP	European Monitoring and Evaluation Programme
Eq	Equation
f-functions	Functions in the stomatal conductance model that accounts for the limiting effects of various environmental factors (e.g. temperature (f_{temp}) and irradiance (f_{light}))
F_{st}	Stomatal flux of O_3 (nmol m^{-2} PLA s^{-1})
g_{ext}	External leaf, or cuticular, conductance
g_{max}	Species-specific maximum stomatal conductance (mmol O_3 m^{-2} PLA s^{-1})
g_s	Stomatal conductance (mmol O_3 m^{-2} PLA s^{-1})
h_0	Phase displacement, defining at what time the daily O_3 concentration maximum and minimum occur in the trigonometric method
m a.s.l.	Meters above sea level
MATCH	Multi-scale Atmospheric Transport and Chemistry modelling system
ME	Modelling efficiency
NMAE	Normalised mean absolute error
PAR	Photosynthetically active radiation
PBL	Planetary boundary layer
PLA	Projected leaf area (m^2), which is the total area of the sides of the leaves that are projected towards the sky
ppb	Parts per billion (the fraction of e.g. O_3 molecules out of a billion air molecules), at normal air pressure and temperature 1 ppb O_3 corresponds to 2 µg O_3 per m^3 air
PPFD	Photosynthetic photon flux density (µmol m^{-2} s^{-1})
POD_Y	Phytotoxic O_3 dose expressed as the accumulated stomatal flux of O_3 above a flux threshold of Y nmol m^{-2} PLA s^{-1} (mmol m^{-2} PLA)
R^2	Coefficient of determination
r_a	Aerodynamic resistance
r_b	Leaf boundary layer resistance
r_c	Leaf surface resistance

RCA3	The Rossby Centre Regional Climate model
RH	Relative humidity (%)
r_s	Stomatal resistance
SWP	Soil water potential (MPa)
T	Air temperature (°C)
UNECE	United Nations Economic Commission for Europe
VOC	Volatile organic compounds
VPD	Vapour pressure deficit (kPa)
WHO	World health organization
yd	Day of year
z	Height above ground (m)
α	Conversion factor to calculate AOT_{12h} from AOT_{24h} used in the Gaussian method
ΔT	Air temperature difference between two heights
μ	Average
σ	Standard deviation

1. Introduction

Ground-level ozone (O_3) is a harmful air pollutant causing reduced crop yield and quality, reduced forest growth and negative effects on human health in large parts of the world (The Royal Society, 2008). The formation, transport and destruction of O_3 in the ambient air are all influenced by weather conditions and climate. Furthermore, weather and climate influence the plant O_3 uptake and thereby the risk of deleterious effects of O_3 on vegetation. Weather is the current state of the atmosphere, while climate summarises the characteristic weather conditions at a site, including long term averages and the frequency of extreme situations. Climate varies on a wide range of spatial scales. The climate of a south-facing slope is very different from the climate of a north-facing slope and has a large impact on the ecosystem structure and function. The climate is also very different in e.g. the Mediterranean region compared to the Nordic countries. Furthermore, climate can change in time. The work summarised in this thesis aims to show that climate influences ground-level O_3 concentrations through a wide range of processes on different spatial and temporal scales. A main focus is how the variation in climate and O_3 concentrations influence the present and future risk of negative impacts of O_3 on vegetation.

O_3 is a natural constituent of the atmosphere. Most of the O_3 in the atmosphere is found in the stratosphere at an altitude of approximately 10–40 km. Here, O_3 protects life at the surface of Earth from the harmful ultraviolet (UV-B) radiation component of the sunlight. O_3 concentrations in the stratosphere have been decreasing as a result of emissions of O_3-destroying substances, but in the troposphere, where O_3 is harmful to humans and vegetation, it has been increasing since the start of the industrialisation. The ground-level O_3 concentrations in Central Europe a century ago averaged 10 ppb and comparison with modern measurements indicate that the O_3 levels have more than doubled (Volz and Kley, 1988) due to increased anthropogenic emissions. Current annual average O_3 concentrations at rural sites in the mid-latitudes of the Northern Hemisphere range between approximately 20–45 ppb (Vingarzan, 2004). Episodes of high O_3 concentrations, often in excess of 100 ppb and sometimes more than 200 ppb, occur in polluted regions under hot and sunny weather conditions (The Royal Society, 2008). A decline in O_3 peak values, mostly relevant for health impacts, has been observed in Europe over the last decades as a result of reduced European emissions. However, there is no corresponding reduction in the long-term average O_3 concentrations more relevant for damage to vegetation (Solberg et al., 2005b). Existing emission controls are insufficient to reduce O_3 concentrations to levels acceptable for human health and environmental protection (The Royal Society, 2008).

1.1 O_3 risk for vegetation

High O_3 concentrations cause visible leaf injury on sensitive species, commonly in the form of small necrotic flecks or stipples on the upper leaf surface. In the absence of visible injury, chronic exposures to O_3 can significantly reduce crop yield, forest growth and modify species composition (Ashmore, 2005).

The negative effects of O_3 on vegetation are more closely related to the uptake of O_3 through the stomata than to the concentration in the ambient air (Emberson et al., 2000b; Pleijel et al., 2004; Karlsson et al., 2007a). The stomata are the small pores on the plant leaf where the gas exchange, of e.g. CO_2, H_2O and O_2, between the interior of the plant and its surroundings take place. Also O_3 can diffuse into the plant when the stomata are open. By varying the width of the stomatal pores a plant is able to control the entry of CO_2 into the leaf and balance it to water loss through transpiration. For example, at a given O_3 concentration, the stomatal flux (O_3 uptake) will be greater under humid conditions since dry air and soil induce stomatal closure to minimize plant water loss through transpiration. In addition to air humidity and soil water availability, also temperature, solar radiation and plant development stage (phenology) influence the degree of stomatal opening. These factors, and not only the ambient O_3 concentrations, therefore have to be considered in risk assessment.

O_3 reduces the yield of a range of crops primarily through reducing photosynthetic rates and accelerating senescence (Ashmore, 2005). O_3 enters the leaf through the stomata and via the production of reactive oxygen species it impairs photosynthetic CO_2 fixation either by impairing the rubisco activity or stomatal functioning and/or indirectly via acceleration of senescence and thus protein (e.g. rubisco) and chlorophyll degradation (Fuhrer, 2009).

A number of O_3 indices have been developed to assess O_3 risk for vegetation. The effect of O_3 exposure on different kinds of vegetation has been established based on experimental data. Exposure systems such as open-top chambers enable plants to be grown under near-natural climatic conditions while the O_3 concentrations are increased by fumigation or decreased by charcoal filtration of the air. The effects considered significant vary between vegetation types and include reduced yield and quality for agricultural crops and reduced growth and accelerated leaf senescence for forest trees. Critical levels are defined as the "concentration, cumulative exposure or cumulative stomatal flux of atmospheric pollutants above which direct adverse effects on sensitive vegetation may occur according to present knowledge" (LRTAP Convention, 2004).

The concentration-based O_3 index AOT40 (concentration accumulated over a threshold concentration of 40 ppb) take into account the external O_3 exposure and require only records of hourly O_3 concentrations. The concentration-based critical levels are suitable for estimating the risk of O_3 damage where climatic data or more advanced models of stomatal O_3 flux are not available (LRTAP Convention, 2004).

The flux-based index POD_Y (phytotoxic O_3 dose above a flux threshold of Y nmol m^{-2} projected leaf area (PLA) s^{-1}) has been developed within the UNECE LRTAP Convention

(LRTAP Convention, 2004; Pleijel et al., 2007), based on the concepts presented in Jarvis (1976), and Emberson et al. (2000a,b). Evaluations have shown the POD_Y index to be superior to the concentration-based index AOT40 in explaining yield reductions for wheat and potato (Pleijel et al., 2004) as well as biomass reductions and visible leaf injury for O_3 sensitive tree species (Uddling et al., 2004; Karlsson et al., 2007a). Unlike the concentration-based index AOT40, the flux-based approach allows modification of O_3 uptake by climatic conditions to be incorporated into the risk assessment. The flux-based critical levels are suitable for mapping and quantifying impacts of O_3 at the local and regional scale, and can be used for assessing economic losses (LRTAP Convention, 2004).

An additional simplified flux-based risk assessment method has been specifically designed for use in large-scale and integrated assessment modelling. It does not involve exceedance of critical levels, but assumes that increasing flux is equivalent to increasing risk. The simplified flux-based methods do not take into account the limiting effect of soil moisture on O_3 flux and can thus be used to indicate the risk under "worst-case" conditions (LRTAP Convention, 2004). Maps of modelled flux-based O_3 risk for a generic crop have been shown to better correspond with field-based evidence of adverse affects compared to AOT40 (Mills et al., 2011).

Even though the flux-based indices are considered more biologically relevant to explain O_3 damage to plants, the AOT40 index is still commonly used in risk assessments because of its simplicity. For example, AOT40 is used within the EU directive (2008/50/EC) on ambient air quality and cleaner air for Europe which is implemented in the Swedish legislation with the Air Quality Ordinance (SFS 2010:477). The strengths and weaknesses of different O_3 indices have been reviewed by Musselman et al. (2006) and Paoletti and Manning (2007).

1.2 Processes that influence O_3 concentrations

1.2.1 O_3 chemistry

O_3 is a secondary air pollutant, which means that it is not emitted as such, but produced in the troposphere from two major classes of precursors; oxides of nitrogen (NO_x = NO + NO_2) and volatile organic compounds (VOCs). In the upper parts of the troposphere carbon monoxide (CO) is also an important precursor. Short-waved sunlight (wavelengths < 420 nm) can split NO_2 through photolysis, which leads to a subsequent formation of O_3:

$NO_2 + h\nu \rightarrow NO + O$ (Reaction 1)

$O + O_2 \rightarrow O_3$ (Reaction 2)

Once formed, O_3 may react with NO:

$O_3 + NO \rightarrow NO_2 + O_2$ (Reaction 3)

Reaction 1–3 may reach a point where NO_2 is destroyed and reformed so fast that a steady-state cycle is established (photostationary state). To build up high O_3 concentrations, the presence of VOCs or CO is required. VOC and CO react with the hydroxyl radical (OH), which produces organo-peroxy (RO_2) and hydro-peroxy (HO_2) radicals.

$RH + OH (+ O_2) \rightarrow RO_2 + H_2O$ (Reaction 4)

$CO + OH (+ O_2) \rightarrow CO_2 + HO_2$ (Reaction 5)

RH denotes an arbitrary hydrocarbon compound e.g. for methane (CH_4) the R in RH represents CH_3. The peroxy radicals oxidise NO to NO_2 without any consumption of O_3 (through Reaction 3), allowing net production of O_3 molecules as the resulting NO_2 molecule photolyses:

$RO_2 + NO \rightarrow NO_2 + RO$ (Reaction 6)

$HO_2 + NO \rightarrow NO_2 + OH$ (Reaction 7)

In the remote troposphere O_3 formation is sustained by the oxidation of CO and CH_4. In regions where human emissions significantly influence the VOC composition of the atmosphere, O_3 formation is driven by much shorter-lived VOCs emitted from biogenic and anthropogenic sources, such as evaporation of solvents and incomplete combustion. Important anthropogenic sources of NO_x are fossil fuel combustion (e.g. traffic) and biomass burning. The amount of O_3 precursor emissions are of course important for the production of O_3. Furthermore, the O_3 formation in the troposphere is dependent on weather conditions (e.g. cloud cover) and regional climate (e.g. more radiation over the Mediterranean region than the Nordic countries).

Chemical loss of O_3 occurs through the photolysis of O_3 (at wavelengths < 320 nm) to produce an excited singlet oxygen atom ($O(^1D)$), which can collide with a water molecule and produce two OH radicals. In remote regions of the troposphere O_3 is also consumed by reactions with HO_2 and OH. A more elaborate description of the complex chemistry of O_3 is given in e.g. Jacob (1999) and Seinfeld and Pandis (2006).

An important process of local O_3 removal is referred to as NO_x titration (Sillman, 1999). It is associated with high levels of NO in areas of large emission density, promoting Reaction 3. Freshly emitted NO_x typically consists of ~90% NO (e.g. Pleijel et al., 2009). Removal of O_3 by Reaction 3 is small compared to the rate of O_3 production in urban and polluted rural areas during meteorological conditions favourable to O_3 formation. However, NO_x titration has a large impact on O_3 concentrations in three situations; night-time, winter and locally close to large emissions sources of NO, such as dense traffic.

1.2.2 Advection

The wind is responsible for horizontal transport also known as advection. Pollutants are transported with the wind from emission sources such as a traffic route, an industry or a city. The average time a pollutant will remain in the atmosphere before it is removed through chemical destruction or other removal processes determines to what extent the pollutant will affect other countries or continents through long-range transport. The lifetime of O_3 ranges from a few days at ground level to weeks in the upper troposphere (Jacob and Winner, 2009). O_3 and its precursors can be carried with the winds over long distances, due to their relatively long lifetime. Episodes of high O_3 concentrations in the Nordic countries are to a large extent due to transport of O_3 and O_3 precursors from elsewhere in Europe, whereas the contribution of domestic precursor emissions are believed to be rather small (Solberg et al., 2005a). Intercontinental transport has been shown to be an efficient process and O_3 production over North America and Asia contribute to the O_3 concentrations observed at surface monitoring sites across Europe (Derwent et al., 2004).

1.2.3 Deposition to the underlying surface

The rate of O_3 destruction at the earth's surface is an important factor determining the O_3 concentrations in the lower atmosphere (Galbally and Roy, 1980). Vegetation and soil represent important pathways by which O_3 is removed from the atmosphere, while water and snow surfaces are rather inefficient O_3 sinks (Fowler et al., 2009).

To describe the transfer of a trace gas or particle from the atmosphere to a surface, a resistance analogue is commonly used (Monteith and Unsworth, 2008), in which the flux of e.g. O_3 is treated as an analogue of electrical current flowing through a network of resistances. First the O_3 molecule must pass the aerodynamic resistance, from the air stream above the canopy and down to leaf level. Next it must cross a thin layer of stagnant air at the leaf surface, the leaf boundary layer resistance. Thereafter the O_3 molecule can either enter the leaf through the stomatal apertures (stomatal resistance), or deposit on the leaf or soil surface (resistance to leaf or soil surface deposition). These two pathways constitute the surface resistance. The resistance analogue is further described in the Appendix of this thesis.

Based on measurements, Galbally and Roy (1980) estimated the median daytime surface resistance to O_3 uptake over grassland and bare soil to be 100 s m^{-1}. The surface resistance of snow and water is about an order of magnitude larger than the daytime land resistance (Galbally and Roy, 1980). O_3 deposition to vegetated surfaces is largely controlled by the leaf area, physiological activity and associated gas exchange of the vegetation. Therefore the deposition velocities (rate of transfer, reciprocal of resistance) observed typically show diurnal and seasonal cycles (Fowler et al., 2009). The deposition velocities tend to be larger during the growing season and during daytime when the stomata are open. Although the stomatal O_3 uptake is an important sink over vegetated surfaces it accounts for only a fraction of the total deposition, typically one to two thirds (Fowler et al., 2009).

1.2.4 Vertical mixing

The lowest level of the troposphere, which is strongly influenced by the Earth surface, is called the planetary boundary layer (PBL). In this layer mixing is generated by frictional drag as the atmosphere (wind flow) moves across the rough surface of the Earth and when air parcels rise from surfaces when heated by the sun. Merely mountainous areas at high altitude are during daytime exposed to the free troposphere, above the PBL.

The degree of mixing and vertical transport of O_3 in the PBL is largely controlled by the prevailing stability conditions. The atmospheric stability conditions can be viewed as the tendency for an air parcel to move vertically, determined by the variation of temperature with height. The temperature of a dry air parcel moving up through the troposphere will decrease with approximately 1 °C per 100 m (dry adiabatic lapse rate), due to the decrease in air pressure with height. If the air parcel is warmer (colder) than the air around, it will be less (more) dense and continue to rise (sink). In *neutral* atmospheric conditions, the actual temperature profile above a location is the same as the dry adiabatic lapse rate and an air parcel has no inherent tendency to either rise or sink. This situation occurs under cloudy and windy conditions. Clouds restrict surface heating and cooling. Wind tends to homogenise the temperature profile towards the adiabatic through vigorous mechanical turbulence. In the *unstable* atmosphere the air temperature decreases faster with height compared to the neutral state and an air parcel which is displaced either upward or downward will tend to continue to move in this direction. These conditions are typical near the ground during sunny days, when the surface is heated by the sun. In the *stable* atmosphere, the air temperature decreases more slowly with height compared to the neutral state and vertical movements of air is inhibited. During very stable conditions the air temperature increases with altitude. This situation is defined as a temperature inversion. Inversions occur for example during clear and calm nights when the atmosphere is cooled from below as a result of surface long-wave radiative cooling. The concept of atmospheric stability is described in more detail in e.g. Oke (1987).

The degree to which the night-time boundary layer stabilises depends on local climate and topography. Valley sites are more prone to nocturnal temperature inversions since cold (dense) air settles in the lowest parts of the landscape (Oke, 1987; Geiger et al., 2003). Wind shelter and screening from the morning and evening irradiance by the surrounding terrain are also important in explaining the lower night-time temperatures in immersed areas compared to elevated sites (Lindkvist and Lindqvist, 1997). The synoptic weather situation is also of importance. Synoptic refers to weather systems typical of mid-latitude cyclones and anti-cyclones, with scales of 100s to 1000s km. In general, increases in cloudiness and wind cause a reduction in the daily range of temperature and reduce extremes of stability (more neutral) (Oke, 1987).

O_3 concentrations generally increase with altitude, mainly because of the lack of chemical loss in the upper troposphere where water vapour and hence HO_x concentrations are low (Jacob, 1999). In addition, deposition to the surface has little influence on the O_3 concentrations in the free troposphere. Close to the ground the vertical O_3 concentration

gradient can be rather steep, as O_3 is removed due to deposition at the surface. Therefore, vertical mixing will result in a downward transport of O_3 from higher O_3-rich air layers.

1.3 Spatial and temporal variation of O_3 concentrations

The processes described in section 1.2 and the influence of climate result in O_3 concentration variation over a wide range of spatial and temporal scales summarised in Figure 1. Ground-level O_3 is generally considered to be a regional scale air pollution problem. However, there are indications of O_3 concentration variation at a much more local scale. Knowledge of the size of the geographical variation in O_3 concentrations between monitoring stations and the size of the area the measurements represent is important for risk assessment of O_3 exposure. Interpolation between monitoring sites with mechanistically relevant prediction variables requires an understanding of the underlying processes causing this local scale variation. Awareness of local scale variation is also important for model validation as regional scale modelled data are compared to point measurements.

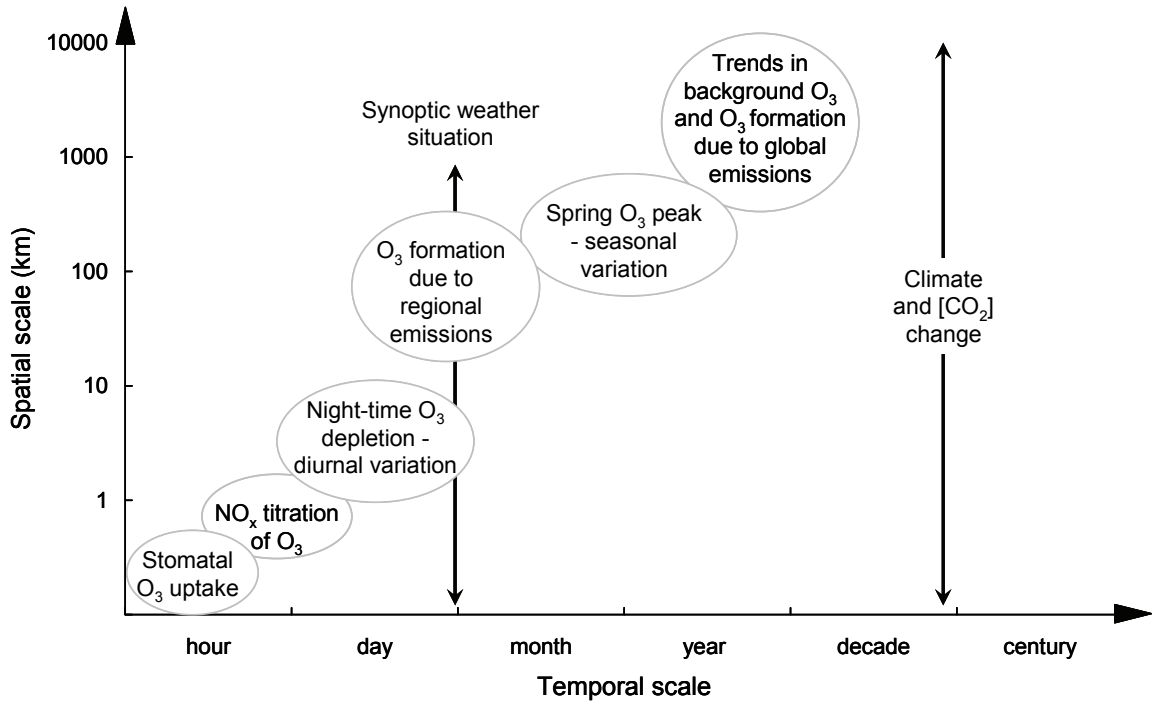

Figure 1. Variation in O_3 concentration on different spatial and temporal scales. The local and regional climate influences the processes causing this variation. The synoptic weather situation as well as potential climate and CO_2 concentration change is of importance over a wide range of scales.

The relative importance of the processes described in section 1.2 varies over the day, resulting in a diurnal cycle in O_3 concentration with a daily maximum and a nightly minimum. At night no photochemical O_3 production occur and the nocturnal decline of O_3

concentrations can be explained by deposition to the ground and vegetation in combination with suppressed vertical mixing due to nocturnal temperature inversions (Garland and Derwent, 1979). The afternoon O_3 concentrations have been shown to be rather similar over wider geographical areas (Coyle et al., 2002).

Several studies have found a relationship between O_3 concentration and altitude, such that sites at higher altitude experience higher O_3 concentrations compared to sites at lower altitude (Ribas and Peñuelas, 2006; Sanz et al., 2007; Gibson et al., 2009). Very few observations have, however, been made of O_3 concentrations in the Scandian Mountain Range, with the exception of some measurements 1987–1994 at Mount Åreskutan, 1250 m a.s.l., in Central Sweden (Bazhanov and Rodhe, 1997).

The degree of night-time O_3 depletion has been found to decrease with altitude (Loibl et al., 1994; Coyle et al., 2002). Coyle et al. (2002) used this relationship when interpolating between measurement sites for O_3 exposure mapping of the UK. Partly in contrast to this, Loibl et al. (1994) argued that similar O_3 maxima was measured at monitoring stations in valleys with different altitude and therefore used relative altitude above the lowest valley ground as an important dependence criterion, when estimating the spatial distribution of O_3 in Austria.

Observations have also shown that the degree of night-time O_3 depletion is smaller at coastal sites compared to sites further inland (Entwistle et al., 1997; Ribas and Peñuelas, 2004). This is related to the low O_3 deposition velocity over water (Galbally and Roy, 1980; Brook et al., 1999) in combination with small diurnal variation in average mixing conditions (Laurila, 1999). The absence of a marked nocturnal decrease in O_3 concentration at coastal sites result in considerably higher average O_3 concentrations compared to inland sites. The inland extent of the enhanced coastal O_3 concentrations is considered to be restricted to a coastal band of only a few kilometres, based on model calculations (Entwistle et al., 1997).

The relative importance of the processes described in section 1.2 also varies over the year, resulting in a seasonal cycle in O_3 concentrations. Because of the photochemical nature of O_3 production, O_3 pollution is to a large extent a spring and summer phenomenon in the temperate zones of the Northern Hemisphere. A pronounced and early spring peak in ground-level O_3 is often observed at high latitudes, e.g. in northern Finland (Hatakka et al., 2003) and northern Sweden (Karlsson et al., 2007b). The fast increase in solar radiation in spring stimulates strong photochemical activity on the arctic winter reservoir of O_3 precursors (Laurila and Hakola, 1996) and enhances vertical mixing of air, compared to the more stable stratification typical of the polar winter, supporting higher ground-level O_3 concentrations (Rummukainen et al., 1996). In addition persistent snow cover influences the O_3 concentrations near the ground since the deposition velocity is very low (Galbally and Roy, 1980), but increases rapidly as the snow disappears and vegetation develops a large, physiologically active leaf area (Rummukainen et al., 1996) with substantial gas exchange, which tends to reduce ground-level O_3.

Many of the processes that form or destroy O_3 as well as cause horizontal and vertical transport of O_3 and O_3 precursors are influenced by the synoptic weather patterns, the regional and the local climate. Climate change is inherently coupled to changes in regional and local meteorology. A change in climate has therefore the potential to influence the O_3 concentrations on a wide range of spatial scales.

1.4 Climate change and O_3

The global average temperature is estimated to have increased by 0.74°C between 1906–2005 and eleven of the last twelve years (1995–2006) rank among the twelve warmest years in the instrumental record of global surface temperature (since 1850). Warming of the climate system is unequivocal and it is very likely that most of the observed increase in global average temperatures since the mid-20th century is due to the observed increase in anthropogenic greenhouse gas concentrations (IPCC, 2007).

Ground-level O_3 concentrations are sensitive to climate change due to the strong dependence on meteorological conditions, (Jacob and Winner, 2009). Modelling studies indicate a significant rise in global average O_3 concentrations in the future unless large emission reductions are implemented (Prather et al., 2003; Dentener et al., 2006; Stevenson et al., 2006). Regional air quality models, simulating the conditions during future climate, generally show increasing O_3 concentrations in Europe despite constant anthropogenic precursor emissions (Meleux et al., 2007; Andersson and Engardt, 2010). The increase is mainly explained by increased temperature, decreased cloudiness (Meleux et al., 2007) and reduced dry deposition (Andersson and Engardt, 2010). Thus, climate change has the potential to counteract emission reductions aimed to limit surface O_3 concentrations.

Elevated CO_2 concentrations have been shown to reduce the stomatal conductance (Ainsworth and Rogers, 2007). Plants do not maximise the CO_2 uptake, but rather optimise the water use efficiency to loose as little water as possible per CO_2 molecule taken up (Jones, 1992). In elevated CO_2 concentrations, the optimum water use efficiency tends to be achieved with smaller stomatal opening. In a case study for winter wheat, Harmens et al. (2007) assumed a 35% reduction in stomatal conductance due to elevated CO_2 concentrations. Current (1997) meteorological conditions and O_3 concentrations was modified and used as input data to POD_6 calculations for five grid squares in the EMEP model of the European Monitoring and Evaluation Programme. The results showed that with a 3°C increase in temperature and constant absolute humidity, the absorbed O_3 dose decreased, despite an assumed 5 ppb increase in O_3 concentrations. The result is, however, based on simplified assumptions of the future climate.

Already in present climate O_3 is considered the most important regional-scale air pollutant causing risks for vegetation and human health in large parts of the world (Fuhrer, 2009), including many developing countries (Emberson et al., 2001). O_3 risks are projected to increase most dramatically in regions with rapid industrialisation and population growth

and with little regulatory action, causing negative impacts on major staple crops and, consequently, on food security (Fuhrer, 2009). In assessing future O_3 risk for vegetation it is important to consider the influence of climate change. Factors such as warming, changes in amount and distribution of precipitation, shifts in growing season and elevated CO_2 concentrations can affect the stomatal uptake of O_3 into the leaves (Harmens et al., 2007). The flux-based POD_Y index allows climatic conditions to modify the estimated plant stomatal uptake rates of O_3, in line with important physiological mechanisms.

2. Aims and hypotheses

The present thesis focused on the spatial and temporal variation of ground-level O_3 concentrations and the impact of present and future climate on the risk of deleterious effects of O_3 on vegetation. O_3 is generally seen as a regional scale air pollution problem, but variation on a smaller scale is considerable. Knowledge of the size of this local scale geographical variation in O_3 concentrations and an understanding of the underlying processes are important in assessments of O_3 exposure. The first aim of the thesis was to describe the variation in O_3 concentration dynamics in Sweden in relation to local scale climate and site characteristics such as altitude, topography, vicinity to the coast and local NO_x emissions.

Due to local scale O_3 concentration variation, permanent O_3 monitoring stations are not always representative for all types of sites within the neighbouring area. A methodology to estimate AOT40 (which is the O_3-index used in the current EU air quality legislation, for the protection of vegetation) from average O_3 concentrations received from e.g. simple and inexpensive passive diffusion samplers could improve the areal coverage of O_3 monitoring and complement existing permanent stations. The second aim was to test two methods of estimating the AOT-index from average O_3 concentrations in combination with information about the O_3 concentration variability.

Site specific meteorological conditions influence both the O_3 concentrations in the ambient air as well as the plant stomatal O_3 uptake. The flux-based approach (POD_Y-index) incorporates the modification of O_3 uptake by climatic conditions into the O_3 risk assessment for vegetation, unlike the still commonly used concentration-based approach (AOT40-index). The third aim was to assess the implications of the local scale O_3 concentration variation in southern Sweden on the flux-based risk of negative effects of O_3 on vegetation.

Already in present climate O_3 is considered to be one of the most important air pollutants in terms of impacts to vegetation and human health. O_3 concentrations are projected to increase in the future in large parts of the world. In combination with rapid population growth and consequently increasing demand for natural resources and food, the future risk for O_3 damage to crops and forests becomes an issue of utmost importance. In assessments of future O_3 risk for vegetation it is especially important to use an approach which considers the influence of climate change, such as the POD_Y-index. The fourth aim was to assess the influence of potential future climate change and elevated CO_2 concentrations on the flux-based risk of O_3 damage to vegetation in Europe.

More specifically the investigated hypotheses were:

1. The O_3 concentration dynamics differ between inland low, inland high and coastal sites in the landscape of southern Sweden. Average O_3 concentrations and diurnal O_3 concentration range (DOR) correlate with site position in the landscape.

2. O_3 concentrations at the alpine site Latnjajaure, in the Scandian Mountain Range, are higher than at northern sites with lower elevation. The spring peak in O_3 is earlier and more pronounced at sites in northern compared to southern Sweden.

3. There is a correlation between DOR and diurnal temperature range (DTR). Differences in both DTR and DOR can to a large degree be explained by the strength of nocturnal temperature inversions.

4. The AOT-index can be estimated from average O_3 data in combination with information on the O_3 concentration variability. The O_3 concentration variability can be estimated from hourly air temperature measurements.

5. The flux-based risk of O_3 damage to vegetation is larger at inland high sites and coastal sites compared to inland low sites.

6. Modelled O_3 concentrations and meteorology for a 50×50 km^2 grid bear stronger agreement with observations at a single site within the grid in well mixed weather conditions compared to situations with calm nocturnal conditions.

7. Climate change can significantly modify the flux-based O_3 risk and the plant stomatal response to elevated CO_2 concentrations has the potential to significantly reduce the O_3 risk.

3. Methods

The spatial variation of O_3 concentrations in the landscape of southwest Sweden was described based on measurements from several field campaigns during the summers 2004–2007 (**Paper I, III, IV**). O_3 concentrations and meteorological parameters were measured using a mobile monitoring station in combination with O_3 and NO_2 concentration measurements with passive diffusion samplers. O_3 and NO_2 concentration measurements with passive diffusion samplers were also performed at an alpine site in the Scandian Mountain Range (**Paper II**) and in the City of Gothenburg. In addition, O_3 concentration data from permanent monitoring stations were analysed.

The risk of deleterious effects of O_3 on vegetation was estimated with the flux-based index POD_Y using an existing method, described in the UNECE CLRTAP Mapping Manual (LRTAP Convention, 2004), to model the stomatal O_3 uptake (**Paper III, V, VI**). The simpler concentration-based index AOT40 is used in current legislation and **Paper IV** investigated methods to estimate AOT40 from average O_3 concentrations, e.g. measured with passive diffusion samplers.

Regional scale chemistry transport models are often used in risk assessments. Modelled O_3 concentrations and meteorological parameters from an EMEP 50×50 km^2 grid-cell were compared to observations from a single site within the grid, to investigate within grid variation of O_3 concentrations and the implications for stomatal uptake of O_3 (**Paper V**). The influence of potential future climate change and increased atmospheric CO_2 concentrations on the flux-based risk of negative effects of O_3 on vegetation in Europe was investigated with modelled future O_3 concentrations from the chemistry transport model MATCH and meteorology from the regional climate model RCA3 (**Paper VI**).

3.1 Measurements and measurement sites

To assess the spatial scale at which O_3 concentration dynamics operates, an exceptionally dense network of monitors is needed (Diem, 2003). The relevant scale to resolve variation in O_3 concentrations depends on the geographic complexity of the area and may change with weather situation. Several studies have indicated a smallest scale of O_3 concentration variation around 3–4 km (Tilmes and Zimmermann, 1998) or 5 km (Diem, 2003). In a study in northern Italy, Gottardini et al. (2010) suggested that a resolution of 1 × 1 km^2 would be appropriate for O_3 concentration modelling. Tabony (1985) concluded that for

temperature the optimum horizontal resolution was rather insensitive to the exact value, but the drop in altitude 3 km from the station, following the valley, was used.

Based on the results from these studies the topography in the vicinity of the sites were characterised by altitude and average altitude within a 3 km radius. Elevation data with 50 × 50 m^2 resolution received from the Digital Map Library was used (**Paper III**). The position in the landscape was represented by the relative altitude, defined as the altitude of the site subtracted by the average altitude within a circle with radius of 3 km centred at the site. There is of course not a clear dividing line between low and high sites, but a continuous range from pronounced valley sites to pronounced hilltop sites. However, for practical purposes the sites where the relative altitude was below 2 are referred to as *inland low* in this thesis. The sites with a relative altitude above 17 m are referred to as *inland high*. Model calculations have indicated that the inland extent of the enhanced coastal O_3 concentrations is restricted to a coastal band of only a few kilometres (Entwistle et al., 1997). Therefore, sites within 4 km from the coastline were defined as *coastal* sites. Location and site characteristics of the rural and urban measurement sites are described in Table 1 and 2.

3.1.1 Mobile monitoring station

A mobile monitoring station was used (**Paper III and IV**) to measure hourly O_3 concentrations and meteorology at sites in southern Sweden (Table 1) with different characteristics such as high (Sandhult, Brobacka) or low (Hedared, Alafors, Lanna) position in relation to the surrounding landscape and vicinity to the coast (Rönnäng, Nidingen, Backåkra). The monitoring station was placed approximately one month at each site during the summers of 2005–2007. O_3 concentrations were measured with an UV-absorption instrument (Thermo Environmental, Model 49) at 5 m height. Air temperature and relative humidity were measured at 1 m (Rotronic Hygroclip S3 RH/T) as well as the temperature difference between 5 and 1 m ($\Delta T_{5\text{-}1}$, Thermocouples type K). The sensors were placed in radiation shields with forced ventilation. Also wind speed (Young Wind Sentry Anemometer) and photosynthetically active radiation (PAR, LICOR, Model Li-190SA) were measured at 1 m height. Wind speed and direction was measured at 5 m (Young Wind Sentry Anemometer & Vane).

3.1.2 Passive diffusion samplers

Measurements of O_3 and NO_2 concentrations were also performed using duplicate passive diffusion samplers (Figure 2) of the Swedish Environmental Research Institute type (Ferm, 2001; Sjöberg et al., 2001) at the same sites as the mobile monitoring station was located (**Paper III, IV**), to compare the O_3 samplers with continuous measurements, extend the O_3 monitoring period and to examine the degree of NO_2 pollution at the respective sites. During the summer of 2004 O_3 concentrations were measured at the inland low site Klevsjön and the inland high site Grytebergen in south-west Sweden 10 approximately one week long measurement periods (**Paper I, III**). During spring and summer 2006–2008, O_3 and NO_2 concentrations were measured at the alpine site Latnjajaure (980 m a.s.l.) in the northernmost part of Sweden (**Paper II**).

Table 1. Coordinates and characteristics of the rural measurement sites. Relative altitude is defined as the altitude of the site subtracted by the average altitude within a circle with radius of 3 km. Values of relative altitude were not available (n.a.) for the sites not included in **Paper III**. MMS = mobile monitoring station, PMS = permanent monitoring station, PS = passive diffusion samplers, met = meteorological conditions.

Site	Latitude	Longitude	Altitude (m a.s.l)	Relative altitude (m)	Characteristics	Measurements
Alafors	57° 56.1' N	12° 7.2' E	37	-2	Inland low, agricultural	MMS; O_3 + met, PS; O_3 + NO_2
Asa	57° 9.9' N	14° 47.0' E	179	-20	Inland low	PMS; O_3
Backåkra	55° 23.3' N	14° 7.9' E	20	n.a.	Coastal	MMS; O_3 + met, PS; O_3 + NO_2
Brobacka	57° 58.8' N	12° 27.6' E	167	46	Inland high, forest	MMS; O_3 + met, PS; O_3 + NO_2
Esrange	67° 52.7' N	21° 3.7' E	485	n.a.	Boreal	PMS; O_3
Grimsö	59° 43.7' N	15° 28.1' E	105	-13	Inland low	PMS; O_3
Grytebergen	57° 58.6' N	12° 21.9' E	176	43	Inland high, forest	PS; O_3
Hedared	57° 48.5' N	12° 44.9' E	191	-11	Inland low, agricultural	MMS; O_3 + met, PS; O_3 + NO_2
Klevsjön	57° 58.8' N	12° 22.7' E	120	-9	Inland low, forest	PS; O_3
Latnjajaure	68° 21.6' N	18° 29.7' E	980	n.a.	Alpine	PS; O_3 + NO_2
Lanna	58° 20.7' N	13° 7.4' E	74	2	Inland low, agricultural	MMS; O_3 + met, PS; O_3 + NO_2
Myrberg	66° 3.8' N	20° 37.3' E	190	n.a.	Boreal	PS; O_3 + NO_2
Nidingen	57° 18.2' N	11° 54.3' E	1	1	Coastal	MMS; O_3 + met, PS; O_3 + NO_2
Nikkaluokta	67° 51.7' N	19° 3.6' E	475	n.a.	Subalpine, near high mountains	PS; O_3 + NO_2
Norra Kvill	57° 48.7' N	15° 33.9' E	251	62	Inland high	PMS; O_3
Norr Malma	59° 49.9' N	18° 37.9' E	16	0	Inland low	PMS; O_3
Palovaara	68° 13.4' N	22° 53.5' E	320	n.a.	Boreal	PS; O_3 + NO_2
Råö	57° 23.6' N	11° 54.9' E	3	6	Coastal	PMS; O_3
Rönnäng	57° 56.2' N	11° 35.0' E	23	11	Coastal	MMS; O_3 + met, PS; O_3 + NO_2
Sandhult	57° 45.6' N	12° 50.5' E	296	38	Inland high, agricultural	MMS; O_3 + met, PS; O_3 + NO_2
Vavihill	56° 1.7' N	13° 9.0' E	168	17	Inland high, forest	PMS; O_3
Vindeln	64° 15.0' N	19° 46.1' E	270	n.a.	Boreal	PMS; O_3
Östad	57° 57.2' N	12° 24.2' E	63	-23	Inland low, agricultural	PMS; O_3 + met

O_3 and NO_2 concentrations were also measured in the urban landscape of Gothenburg (Table 2) during five 5-day periods in February 2005 at eight different locations. Six sites were located close to a major traffic route with varying distance to the heavy traffic, one site was co-located with a permanent urban rooftop monitoring station (Femman) and one site was a rural reference situated about 25 km north-east of the Gothenburg City centre. O_3 and NO_2 concentrations were also measured during five one-week periods 24 July to 28 August 2007 at five locations. In addition to the urban rooftop site Femman and the site closest to the major traffic route, measurements were also performed in an urban park and at two suburban sites.

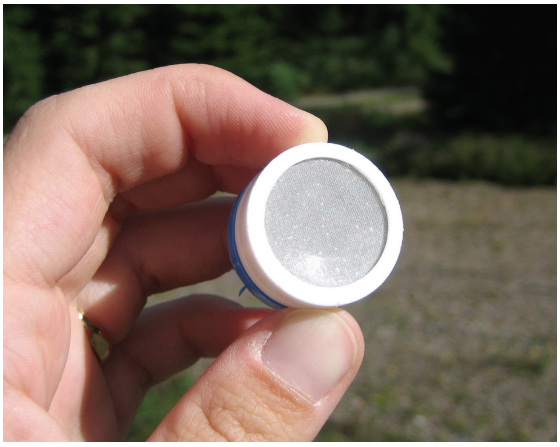

Figure 2. O_3 passive diffusion sampler of the Swedish Environmental Research Institute type.

Table 2. Coordinates and characteristics of the urban measurement sites (PS = passive diffusion sampler, PMS = permanent monitoring station, met = meteorological conditions).

Site	Coordinates	Measurements	Characteristics
Femman	57° 42.52' N 11° 58.24' E	PMS; O_3 + NO_2 + met PS; O_3 + NO_2, Feb 2005 + July-Aug 2007	Rooftop monitoring site (30 m above street level)
Skansen Lejonet	57° 42.85' N 11° 59.35' E	PS; O_3 + NO_2, Feb 2005	15 m above ground, ~200 m west of traffic route
Mast	57° 42.94' N 11° 59.55' E	PS; O_3 + NO_2, Feb 2005	~100 m west of traffic route
Road	57° 42.96' N 11° 59.57' E	PS; O_3 + NO_2, Feb 2005 + July-Aug 2007	Closest (~8 m) to traffic route
Olskroken	57° 42.83' N 11° 59.70' E	PS; O_3 + NO_2, Feb 2005	~15 m east of traffic route
Railroad	57° 42.71' N 11° 59.83' E	PS; O_3 + NO_2, Feb 2005	~20 m east of traffic route and ~400 m south
Lunden	57° 42.70' N 12° 00.03' E	PS; O_3 + NO_2, Feb 2005	Vegetated hillslope, ~200 m east of traffic route
Annekärr	57° 51.90' N 12° 19.08' E	PS; O_3 + NO_2, Feb 2005	Rural reference
Slottsskogen	57° 41.02' N 11° 56.15' E	PS; O_3 + NO_2, July-Aug 2007	Large urban park
Frölunda	57° 39.37' N 11° 55.99' E	PS; O_3 + NO_2, July-Aug 2007	Urban residential area
Björkekärr	57° 43.03' N 12° 2.58' E	PS; O_3 + NO_2, July-Aug 2007	Suburban residential area

The passive diffusion sampler technique is based on molecular diffusion of gases. The gas molecules diffuse into the sampler to a sorbent where they are quantitatively collected. Analysing the sorbent (in this case at the Swedish Environmental Research Institute accredited laboratory) gives a concentration value integrated over time. Turbulent diffusion inside the sampler is avoided by using a membrane at the inlet. Passive diffusion sampling has been used in Sweden (Ferm and Svanberg, 1998; Svanberg et al., 1998), UK (Stevenson et al., 2001), Canada (Gilbert et al., 2003) and many other parts of the world (Ferm and Rodhe, 1997; Ayers et al., 1998; Carmichael et al., 2003). Passive diffusion samplers are small, light, cost-efficient, soundless, do not require electricity and therefore geographically flexible. The technique is used to increase the spatial resolution of measurements, to complement permanent monitoring stations and to evaluate monitoring site locations accordingly, at low cost. The drawback of passive diffusion samplers is the limited time resolution (approximately 1 week to 1 month, depending on the degree of pollution). Several studies have described and evaluated the passive diffusion sampling technique in detail (e.g. Ferm and Svanberg, 1998; Ferm, 2001; Yu et al., 2008; Vardoulakis et al., 2009).

Comparison between the parallel measurements of O_3 concentrations with passive diffusion samplers and continuously measuring UV-absorption instruments performed in this study showed that the passive diffusion samplers satisfactorily represented the average concentration during the measurement periods (Figure 3). Due to deposition towards the earth surface there is a steep vertical gradient in O_3 concentration close to the ground. The passive samplers were placed at 2 or 3 m height while the air inlet for the UV-instrument was at 5 m. The difference in measurement height was corrected for according to a method in Mapping Manual (LRTAP Convention, 2004), suggesting that the O_3 concentrations at 3 m was 98% of the 5 m concentrations and that the O_3 concentrations at 2 m was 96% of the 5 m concentrations.

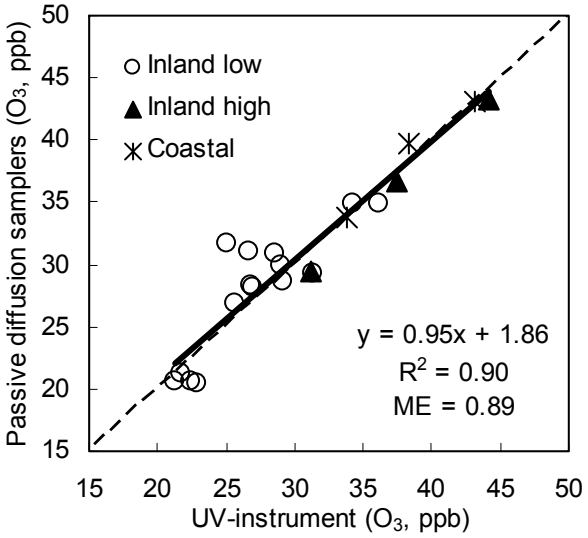

Figure 3. Comparison of O_3 concentrations measured with passive diffusion samplers of Swedish Environmental Research Institute type and parallel measurements with UV-absorption instruments (the mobile monitoring station or at Östad). Solid black line is linear regression, dashed black line is y = x and ME is modelling efficiency. N=21 measurement periods.

3.1.3 Permanent monitoring stations

In addition to the above described measurements, data from several permanent monitoring stations have also been analysed (Table 1). A key location was the monitoring site Östad, which was used as a reference site. Östad is situated 45 km northeast of Gothenburg, in southwest Sweden. It is an agricultural site, characterised by large areas of low vegetation, situated in a broad valley (ca 1 km) surrounded by a forested, hilly landscape. At Östad the hourly O_3 concentrations were measured with an UV-absorption instrument (Thermo Environmental, Model 49) at 5 m height, temperature and relative humidity (Rotronic Hygroclip) at 1 m height enclosed in reflective radiation shields with forced ventilation, as well as the temperature difference between 9 and 1 m ($\Delta T_{9\text{-}1}$, Thermocouples type K). Wind speed (Young Wind Sentry Anemometer & Vane) was measured at 9 m height and PAR (LICOR, Model Li-190SA) at 1 m height.

Furthermore, hourly O_3 concentration data was received from several rural permanent monitoring stations in Sweden. Esrange, Vindeln Grimsö, Norra Kvill, Råö and Vavihill are operated within the Swedish national O_3 monitoring network and are part of the European Monitoring and Evaluation Programme (EMEP, data available at www.ivl.se). Norr Malma is part of Stockholm and Uppsala County Air Quality Management Association (data available at slb.nu/lvf). Asa is an experimental forest and research station at the Swedish University of Agricultural Sciences (asa.esf.slu.se) also financed by the Regional Air Quality Protection Associations in Kronoberg and Jönköping Counties. Measurements of O_3 concentrations and meteorology at the urban site Femman in Gothenburg City centre were also used. The Femman site is situated at the roof of a 30 m tall building (the general height of the taller buildings in the city centre) and is operated by the Environmental Administration in the City of Gothenburg.

At Nikkaluokta, Palovaara and Myrberg monthly measurements of O_3 and NO_2 with passive diffusion samplers are performed as part of the Swedish Throughfall Monitoring Network (SWETHRO, data available at www.ivl.se).

3.2 Assessment of O_3 risk for vegetation

3.2.1 The AOT40 index

The concentration-based O_3 index AOTX (accumulated O_3 above a concentration threshold of X ppb) is calculated as the sum of the difference between the hourly O_3 concentrations at vegetation height and the threshold concentration X ppb for all daylight hours within a specified time period.

In **Paper IV**, two different methods to estimate AOT-indices with different threshold concentrations from the average O_3 concentrations in combination with information about the O_3 concentration variability were tested. The O_3 concentration variability was

calculated from parallel hourly air temperature measurements in combination with a statistical relationship between O_3 and temperature variability.

The Gaussian method was developed by Tuovinen (2002) and assumes that the hourly O_3 concentrations (C) have a Gaussian probability density function f(C) with mean μ and standard deviation σ. The AOT-index with threshold concentration X ppb can then be calculated based on the average O_3 concentrations from e.g. a passive diffusion sampler in combination with an estimate of σ. 24-hour AOT values are yielded from the Gaussian method. However, 12-hour daytime AOT values are more relevant for risk assessment of O_3 damage to vegetation since plant O_3 uptake is considerably lower during night compared to daytime. 12-hour AOT can be calculated from 24-hour AOT by the use of a conversion factor (α).

The trigonometric method is similar to the method developed by Loibl et al. (1994) and later applied by Gerosa et al. (2007). The diurnal variation in O_3 concentrations is represented by a sine function with amplitude (A) that is half the DOR, oscillating around the average O_3 concentration. The sine-function is synchronised with the O_3 concentration diurnal pattern by a phase displacement (h_0), defining at what time the O_3 concentration minimum and maximum occur. Essentially, AOT is calculated for one average day and then multiplied by the number of days the monitoring was in progress.

The measurements at Nidingen, Rönnäng, Backåkra, Sandhult, Brobacka, Lanna, Hedared, Alafors and Östad were randomly divided between a parameterisation dataset and a validation dataset and split into weekly periods. The parameterisation dataset was used to calculate the site-type specific parameter α in the Gaussian method and h_0 in the trigonometric method. For each weekly period in the validation dataset, the AOT-index was estimated from the weekly average (mimicking the result of a passive diffusion sampler) using the two described methods and calculated from hourly O_3 concentration data as conventional. To quantify the fit between the estimated and measured values, modelling efficiency (ME) and normalized mean absolute error (NMAE), both described by e.g. Janssen and Heuberger (1995), were used. The ME value is a measure of the relative improvement of the estimates compared to the average of the observed values. The NMAE can be interpreted as the average overestimation (positive or negative), given in relation to the average of measured AOT. A perfect fit would have all data points arranged on the 1:1 line, an ME value of 1 and a NMAE of 0%. The calculation of the concentration-based AOTX-index with the Gaussian and trigonometric methods are further described in **Paper IV** and in the Appendix of this thesis.

3.2.2 The POD_Y index

The stomatal O_3 flux was calculated using the multiplicative algorithm given in the UNECE CLRTAP Mapping Manual (LRTAP Convention, 2004). It includes functions accounting for the limiting effects of various factors, such as O_3 concentrations, plant development stage (phenology), irradiance, temperature, water vapour pressure deficit (VPD) and soil water potential (SWP) on stomatal O_3 uptake. The functions (f_{O3}, f_{phen},

f_{light}, f_{temp}, f_{VPD} and f_{SWP}) are expressed in relative terms (take values between 0 and 1) as a proportion of the species-specific maximum stomatal conductance, thereby regulating the O_3 flux into the plant leaf. The phytotoxic O_3 dose above a flux threshold Y nmol m^{-2} PLA s^{-1} (POD_Y) is then accumulated over a period of time corresponding to the growing season, when the plant is considered to be sensitive to O_3. The multiplicative algorithm and its parameterisation are described in detail in the UNECE CLRTAP Mapping Manual (LRTAP Convention, 2004) and in the Appendix of this thesis.

Models of stomatal conductance have been parameterised for a limited number of crop and tree species. In **Paper V**, the phytotoxic O_3 dose was calculated for wheat and potato (POD_6). However, soil water potential was assumed not to be limiting in the area considered in this study, where droughts are rare and irrigation of arable land not common practice.

A simplified multiplicative stomatal conductance model was used to indicate the degree of risk for O_3 damage to a generic crop (POD_{3crop}, **Paper III, VI)** and generic deciduous tree species ($POD_{1.6tree}$, **Paper VI)** (LRTAP Convention, 2004; Simpson and Emberson, 2006). The simplified flux method is intended to be used within large-scale modelling. Important simplifications are that O_3-induced premature senescence is assumed to have no effect on stomatal conductance (i.e. f_{O3} =1) and a lower threshold is used for the generic crop than recommended for specific crops, making the method numerically more robust (Tuovinen et al., 2007). For a generic crop a three month time-window for stomatal O_3 flux accumulation is used to bypass the uncertainty in the timing of the relevant time-interval, which, especially for crops, is rather short. Due to uncertainties caused by difficulties in modelling a plant-relevant SWP, the potentially large variations in soil moisture within a model grid and possible irrigation practices, soil moisture is assumed not to limit stomatal conductance (i.e. f_{SWP} = 1). However, in one $POD_{1.6tree}$ calculation a SWP function was included to estimate the potential influence of this factor on the stomatal O_3 flux **(Paper VI)**. It was assumed that water was freely available from 0 to -0.05 MPa SWP with a linear decrease in water availability (and stomatal conductance) below -0.05 MPa down to a minimum at -1.5 MPa SWP (Hall et al., 1977).

In **Paper VI**, a CO_2 response function (f_{CO2}) for a generic crop and a generic deciduous tree was parameterised based on experiments found in the literature where crops and trees grown in elevated CO_2 concentrations responded with reduced stomatal conductance. The influence of increasing CO_2 on stomatal conductance was assumed to linearly decrease between 360 and 560 ppm CO_2 concentration from 1 to 0.66 for a generic crop and to 0.8 for a generic deciduous tree, with no further reductions in stomatal conductance above 560 ppm CO_2. There is however, a large uncertainty with respect to the effect of elevated CO_2 on stomatal conductance in closed forest stands (Uddling et al., 2008; Uddling et al., 2009). $POD_{1.6tree}$ was therefore calculated both with and without the inclusion of the stomatal CO_2 response function. This was done also for the generic crop in order to separate effects of climatic changes from effects of rising CO_2 concentrations on stomatal O_3 flux.

3.3 Chemistry transport models

3.3.1 EMEP

To investigate within grid variation of O_3 concentrations and the implications for stomatal uptake of O_3, measurements at Östad were compared to the corresponding data from the grid in the EMEP photo-oxidant model in which Östad is situated (56, 61; official EMEP coordinates, **Paper V**). The EMEP model is the Eulerian chemistry transport model (CTM) of the European Monitoring and Evaluation Programme (EMEP). It is primarily designed for large-scale modelling of O_3 over the whole of Europe and is used as a tool within the European air pollution abatement strategy and legislation work (Berge and Jakobsen, 1998; Simpson et al., 2003a; Fagerli et al., 2004).

An O_3 dry deposition module (DO_3SE; Deposition of O_3 and Stomatal Exchange) has been incorporated within the EMEP model to calculate O_3 fluxes (Emberson et al., 2000a; Simpson et al., 2001, 2003a,b). For deposition modelling, each grid is divided into a number of land use categories (e.g. temperate crops, temperate coniferous forests). The vegetation characteristics such as height and leaf area index of each sub-grid land use are used to calculate "local" values of atmospheric stability and near-surface humidity. These values are used to calculate canopy conductance, vertical O_3 concentration gradients and deposition flux of O_3 to both stomata and non-stomatal surfaces (Simpson et al., 2001, 2003b). The procedure aims to capture some of the characteristics of different vegetation types within a grid, but is of course limited by the 50 km grid-size of the original data.

3.3.2 MATCH

To assess the influence of climate change and elevated CO_2 concentrations on the flux-based risk of O_3 damage to vegetation in Europe, O_3 concentrations from the regional chemistry transport model MATCH were used (**Paper VI**). MATCH is described in detail by Robertson et al. (1999). MATCH was driven by meteorology from the Rossby Centre's regional climate model (RCA3), which is described in Kjellström et al. (2005) and Jones et al. (2011). RCA3 was forced with climate data from the ECHAM4/OPYC3 global model on its boundaries, simulating the IPCC SRES A2 and B2 emission scenarios (Nakicenovic et al., 2000). A2 is one of the more pessimistic greenhouse gas emission scenarios. Anthropogenic emissions and boundary trace concentrations were held constant, representing the year 2000, in order to limit the investigation to the influence of climate change (and not changes in emission patterns). Emissions of biogenic isoprene are calculated online in MATCH, but natural emissions of other VOCs, sulphur or nitrogen containing compounds are not included in the present set-up. Hence, changes in photochemistry, transport patterns, emissions and uptake by vegetation affect modelled future O_3 concentrations. Three 30-year periods were simulated: reference (1961–1990), near future (2021–2050) and far future (2071–2100). The set-up of the model system is further described in Andersson and Engardt (2010).

The canopy-scale O_3 dry deposition to vegetation is a function of temperature, air humidity, soil moisture, and irradiance in MATCH. For risk assessment purposes it is the stomatal O_3 flux to the sunlit leaf level of specified vegetation types that is important and not the canopy-scale flux. Ten monitoring sites within the European Monitoring and Evaluation Programme (EMEP) were selected in transect from northeast (northern Finland, FI22) to southwest (southern Spain, ES07) to represent different climatic conditions in Europe. The flux-based O_3 risk (POD_Y) was calculated off-line for a generic crop and a generic deciduous tree at the ten sites based on modelled data from the corresponding grid-cell in MATCH (O_3) and RCA3 (meteorology). The location and characteristics of the sites are further described in **Paper VI.** To test if average POD_Y for the far future (A2 emission scenario) was significantly different compared the reference period, a two-sided Student's t-test was applied, assuming unequal variances.

4. Results

4.1 O_3 concentration variation in Sweden

Average O_3 concentrations were found to vary considerably over small distances. As an example, a 5 ppb difference in average summer O_3 concentration was measured between two sites (Grytebergen and Östad) only 3 km apart, but with high or low position in relation to the surrounding local terrain (**Paper I**). Also the diurnal dynamics of O_3 differed substantially between sites situated low or high in the inland or in the vicinity of the coast (**Paper I, III, IV**). Figure 4 shows an example of the average diurnal O_3 concentrations at two inland low sites (Östad and Asa), two inland high sites (Vavhill and Norra Kvill) and one coastal site (Råö). Figure 4 is based on hourly O_3 concentration measurements at permanent monitoring stations in southern Sweden during April to September 2007–2009 (on average 1.1% data loss, maximum 3.1% at Vavihill). The inland low sites had a more marked nocturnal O_3 decrease resulting in nearly twice as large diurnal O_3 concentration range (DOR, 21.3 ppb) compared to the inland high and coastal sites (11.0 and 11.3 ppb, respectively). The average daytime (hour 8–20) O_3 concentrations were similar between sites, however largest at the coastal site (38.0 ppb at the coastal site, 35.6 ppb at the inland low sites and 36.7 ppb at the inland high sites).

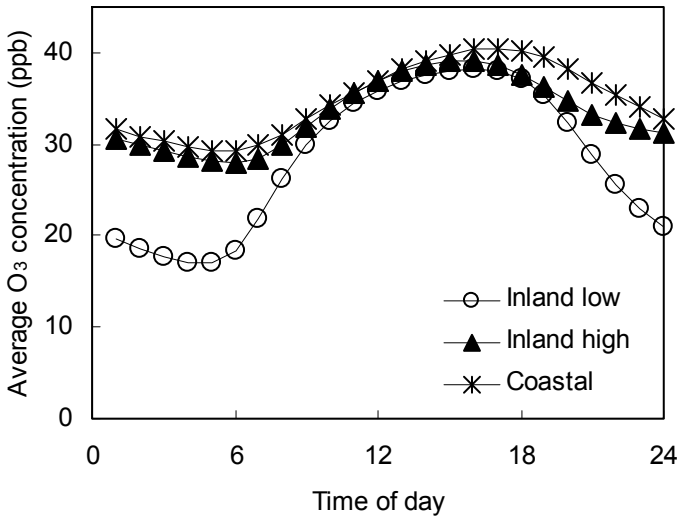

Figure 4. Average diurnal O_3 concentrations at the inland low sites Östad and Asa, the inland high sites Vavihill and Norra Kvill and the coastal site Råö during April–September 2007–2009 (local time).

Based on the measurements with the mobile monitoring station at Lanna, Hedared, Brobacka, Sandhult, Nidingen and Rönnäng, the largest diurnal variation in both O_3 concentrations and temperature was measured at the inland low sites (on average 27 ppb and 12°C) while inland high and coastal sites had smaller DOR and DTR (on average 19 ppb and 8°C at the inland high sites; 17 ppb and 5°C at the coastal sites). A statistically significant relationship between DOR and DTR was found (p=0.001), where DTR explained 39% of the variance in DOR (**Paper III**). Since the daytime difference in O_3 concentrations between sites are smaller than those at night, night-time conditions, particularly nocturnal temperature inversions, which in turn limit vertical O_3 transport, may explain a large part of the relationship between DTR and DOR. Site average DOR was strongly correlated with site average maximum nocturnal $\Delta T_{5\text{-}1}$ (R^2=0.98, p<0.001), as can be seen in Figure 5 (**Paper III**). A statistically significant non-linear relationship (R^2 = 0.74, p<0.001) was also found between DTR and maximum nocturnal $\Delta T_{5\text{-}1}$ at six sites (N = 212 days).

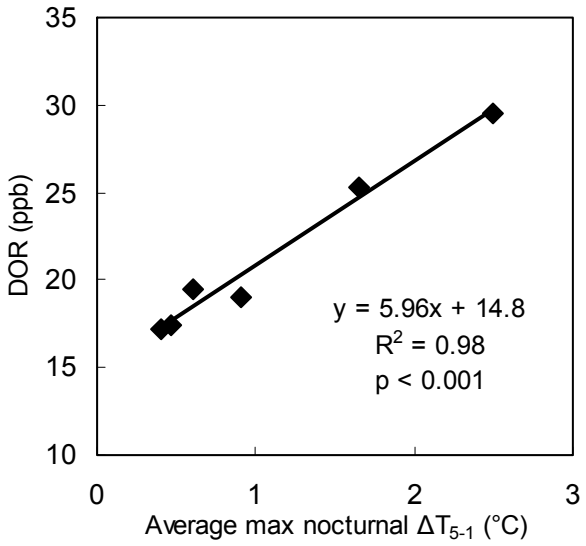

Figure 5. Average diurnal O_3 concentration range (DOR) in relation to the average maximum nocturnal $\Delta T_{5\text{-}1}$ for the sites Nidingen, Rönnäng, Brobacka, Sandhult, Lanna and Hedared.

4.1.1 Coastal climate

Nidingen is an isolated, small and low island situated 6 km from the west coast of Sweden. During an approximately six week long measurement period (15 April to 7 June 2007) the average diurnal curves at Nidingen, showed a difference of up to 5 ppb compared to the inland low site Östad in daytime, and much larger differences during night-time (**Paper III**).

To investigate the influence of advection of marine O_3-rich air, Nidingen was compared to the coastal permanent monitoring station Råö in relation to wind direction (Figure 6a). Råö is located approximately 10 km from Nidingen on the west coast of Sweden. The difference in O_3 concentrations between Nidingen and Råö was calculated as (Nidingen-Råö)/Nidingen. The difference was clearly largest in easterly wind directions, with air coming from the inland. The largest average difference in O_3 concentration was 17% for the 45° wind sector centred around 90° (east). The difference was smaller in south and

westerly wind directions, when the air came from the open sea. The lowest average difference was 6% for the 45° wind sector centred around 180° (south). Based on the direction of the coastline it was assumed that the open sea would have most influence on the O_3 concentrations at both sites in wind directions of 205–295° (from the open sea). In wind directions of 25–115° (from the inland) Råö is likely more influenced by inland air while the island Nidingen is still characterised by marine air. The average difference in O_3 concentrations between Nidingen and Råö was 15% during north-easterly winds and 9% during south-westerly winds (Figure 6b). The difference in O_3 concentrations between the two wind sectors was statistically significant ($p<0.001$).

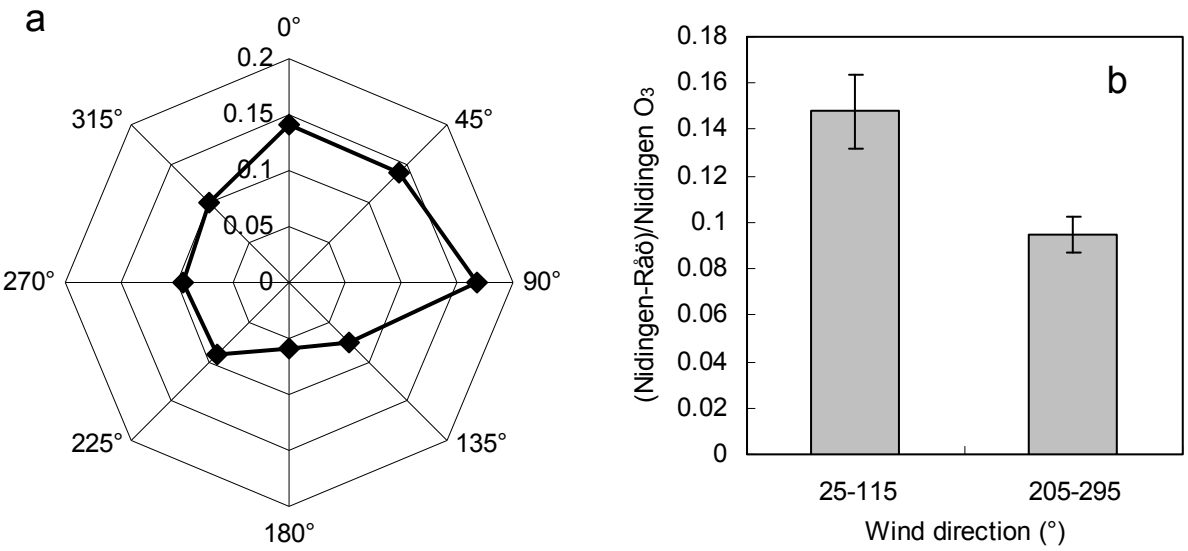

Figure 6. (a) The difference in O_3 concentrations between Nidingen and Råö ((Nidingen-Råö)/Nidingen) in relation to wind direction. (b) The difference in O_3 concentrations between Nidingen and Råö ((Nidingen-Råö)/Nidingen) between wind directions of 25–115° (from the inland) and wind directions of 205–295° (from the open sea). Error bars show 95% confidence intervals of the mean, N = 222 and 342 hours respectively.

4.1.2 Topography and altitude

Focusing only on inland sites, topography is important for the formation of nocturnal temperature inversions. In **Paper III** the average O_3 concentrations and DOR was therefore related to relative altitude. Since the mobile monitoring station could only measure at one site at the time, the O_3 concentration measurements from each of the different sites were normalised by dividing with the simultaneous measurements from the permanent monitoring station Östad, hence used as a reference site for all measurement periods. The normalised values are denoted $[O_3]_{site:Östad}$ and $DOR_{site:Östad}$.

Figure 7a shows a statistically significant relationship between the average $[O_3]_{site:Östad}$ and relative altitude (R^2=0.94, p=0.002). Sites located high compared to the surrounding landscape experienced higher average O_3 concentrations than sites positioned low. The corresponding relationship between average $[O_3]_{site:Östad}$ and altitude was not statistically significant (R^2=0.38). To increase the number of sites, Grytebergen and Klevsjön were included in Figure 7a. Only site average O_3 concentrations and not DOR could be

calculated at these two sites, since the O_3 concentrations were measured with passive diffusion samplers. Therefore Grytebergen and Klevsjön were not included in Figure 7b, which shows that the average $DOR_{site:Östad}$ correlated with relative altitude (R^2=0.87, p=0.015). Sites positioned high compared to the surrounding landscape had a smaller diurnal variation in O_3 concentrations than sites with a low position. The corresponding relationship between average $DOR_{site:Östad}$ and altitude was not statistically significant (R^2=0.64).

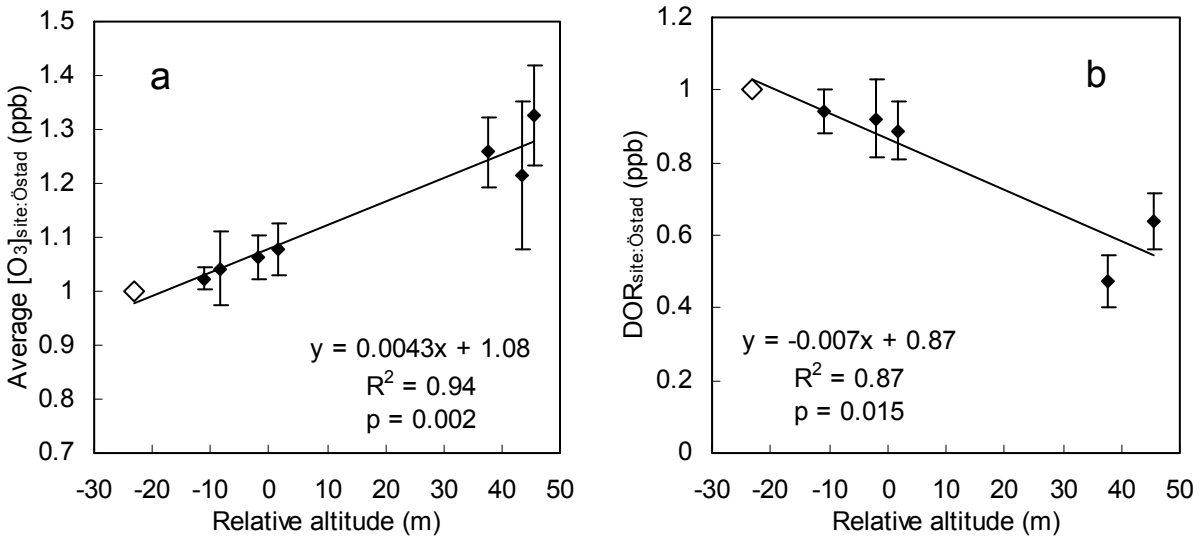

Figure 7. Average O_3 concentrations (a) and average diurnal O_3 concentration range (DOR) (b) at each site, normalised by dividing with the simultaneous measurements from the continuous monitoring station Östad, in relation to relative altitude. Error bars show 95% confidence intervals of the mean, N = 24–42 days. The sites are Hedared, (Klevsjön), Alafors, Lanna, Sandhult, (Grytebergen) and Brobacka. The open diamond represents the reference site Östad.

Very few measurements of O_3 concentrations have been made at high altitude in the Scandian Mountain Range. O_3 concentration was therefore measured with passive diffusion samplers at the alpine site Latnjajaure (980 m a.s.l.) in northernmost Sweden and compared to the closest permanent monitoring station with hourly O_3 concentration measurements, Esrange. Esrange is located approximately 120 km southeast of Latnjajaure at lower altitude (485 m a.s.l.). The O_3 concentrations were higher at Latnjajaure compared to Esrange during thirteen out of fifteen measurement periods. The difference was significant ($p<0.01$) based on a nonparametric sign test. The largest difference between Latnjajaure and Esrange was 4.9 ppb and occurred during a two-week measurement period in the end of August 2007.

4.1.3 Seasonal variation in O_3 concentrations

Figure 8 shows the yearly cycle in ground-level O_3 concentrations at five sites in northern Sweden compared to three sites in southern Sweden (**Paper II**). Each point represents a five-year average for the respective months of the year. All the sites in the north exhibited a seasonal cycle with a pronounced, high and early peak in O_3 concentration. Maximum O_3 concentrations were observed in April at all the northern sites, while the maximum

was in May at Råö and Vavihill in the south of Sweden. During summer (June–August) O_3 concentrations were significantly higher at the southern sites than at the northern sites. The spring peak (monthly average) was higher at three of the northern sites compared to Råö with a maximum of 41 ppb. The highest concentrations were obtained in Nikkaluokta with 49 ppb as the April average and, unlike the other sites, a monthly maximum well above 60 ppb. The lowest spring peak in Norrbotten County, 40 ppb in April and similar in magnitude to the May maximum at Råö, was observed at Myrberg. The seasonal cycle of ground-level O_3 at Vindeln was similar to Myrberg with a maximum in April of 41 ppb. The summer O_3 concentrations at Norra Kvill were similar to the other two sites in southern Sweden (Råö and Vavihill). The spring peak did however occur in April, but was less pronounced compared to the three northernmost sites. Compared to Råö and Vavihill, Norra Kvill is situated at higher altitude and most likely experiences more frequent snow cover during winter.

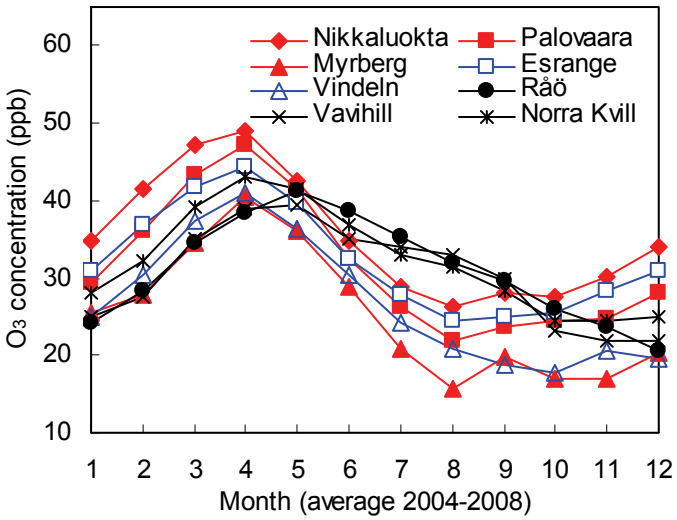

Figure 8. Seasonal variation in O_3 concentration at five sites in northern Sweden and three sites in southern Sweden. The monthly values represent the average for each month of the year during the period 2004–2008.

4.1.4 O_3 in urban air

Measurements of O_3 and NO_2 concentrations with passive diffusion samplers in the urban landscape revealed a large variation in concentration. The 25-day winter average of NO_2 was 13.1 ppb at the urban rooftop monitoring site Femman, while 24.7 ppb at a site directly beside a major traffic route. The NO_2 concentration at a rural site was much lower compared to the urban sites, only 3.1 ppb. The O_3 concentrations were approximately 30% lower at the most NO_2 polluted site compared to Femman (18.5 ppb compared to 28.7 ppb). The average O_3 concentrations during the five weeks of summer measurements were relatively low, ranging from 19.7 ppb at the most NO_2 polluted site close to the traffic route (19.0 ppb NO_2) to 29.5 ppb at the urban park site (4.0 ppb NO_2). The weather conditions during the summer measurements were dominated by low air pressure, low temperatures (on average 17 °C) and rain. These weather conditions do not promote high O_3 concentrations and are most likely the explanation to the measured low O_3 concentrations during the summer compared to the winter.

The NO_2 concentrations were largest at the site closest to the major traffic route, a large emission source of NO_x, and decreased with distance from the heavy traffic. The O_3 concentration variation in the urban landscape had the opposite pattern with a marked reduction in concentration at the sites with high NO_2 concentrations. Figure 9 shows a statistically significant negative linear relationship between the O_3 and NO_2 concentrations ($p<0.001$) during both the summer and winter measurements. The reduction in O_3 concentrations at NO_2 polluted sites can be attributed to NO titration.

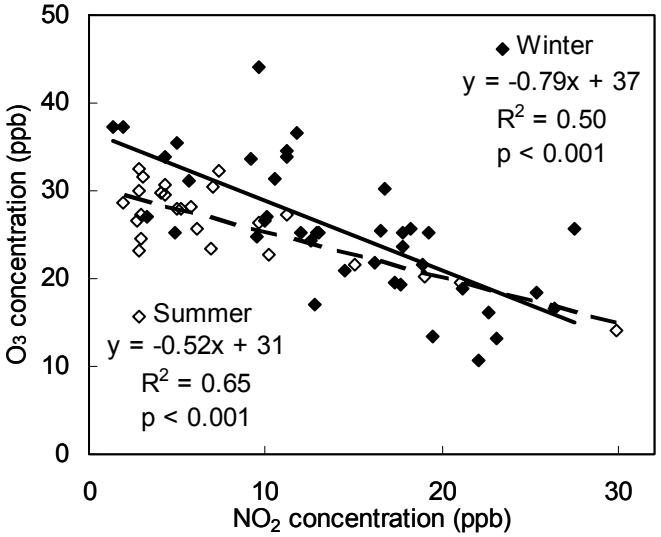

Figure 9. O_3 concentrations in relation to NO_2 concentrations during 5 five-day measurement periods at eight locations in February 2005 and 5 seven-day measurement periods at five locations in July–Aug 2007. The O_3 and NO_2 concentrations were measured with passive diffusion samplers.

4.1.5 Synoptic weather situation

The degree of spatial variation in O_3 concentrations depends to a large degree on synoptic weather situation. The largest difference in O_3 concentrations between sites generally occurred under high pressure weather situations (**Paper III**). The difference in weather conditions between situations with large and small site differences in O_3 concentrations were demonstrated in **Paper I**. The rate of temperature change with time at Grytebergen, Klevsjön and Östad as well as wind speed and $\Delta T_{9\text{-}1m}$ at Östad for three days with small difference in O_3 concentrations between sites were compared to three days with large difference in O_3 concentrations. During the time period with small differences in O_3 concentrations between sites the winds speed also varied little and never approached zero. The $\Delta T_{9\text{-}1m}$ was small and the rate of hourly temperature change small and similar between the sites. In contrast to this, during the time period with large differences in O_3 concentrations between sites the diurnal variation of temperature and $\Delta T_{9\text{-}1m}$ was very pronounced at Östad. Also, wind speed approached zero during large parts of the night. In the evening and early night the rate of temperature change revealed a much faster cooling at the inland low sites Östad and Klevsjön compared to the inland high site Grytebergen, indicating a fast development of temperature inversions at the inland low sites.

In **Paper V** the agreement of O_3 concentrations and temperature between the EMEP model and measurements at Östad was investigated in relation to synoptic weather situation. The data were divided into days with low (<0.5 m s^{-1}) and higher (>0.5 m s^{-1})

measured average nocturnal wind speed (21:00–4:00 local time). Significant differences between modelled and measured O_3 concentrations and temperature were not found during daytime regardless of weather situation. During calm nights the O_3 concentrations and temperature were clearly overestimated by the EMEP model. In calm nocturnal conditions, most likely associated with anti-cyclonic weather situations local, site-specific conditions at Östad are most pronounced and the measurement site not representative of the grid taken as a whole.

4.2 Estimation of AOT40 from average O_3

The strength of nocturnal temperature inversions influences the diurnal dynamics of both O_3 concentrations and air temperature. Based on the 22 weekly periods in the parameterisation dataset, linear statistically significant relationships between the standard deviations in O_3 concentration and air temperature ($y=1.88x+3.04$, $R^2=0.73$, $p<0.001$, to be used in the Gaussian method) and between the weekly averages of DOR and DTR ($y=1.75x+8.86$, $R^2=0.76$, $p<0.001$, to be used in the trigonometric method) were found (**Paper IV**).

Both the Gaussian and trigonometric methods estimated 24-hour AOT with low threshold concentrations with high accuracy. As the threshold concentrations were increased above the average O_3 concentration (34 ppb) there was a rapid decline in modelling efficiency. However, for AOT40, the modelling efficiency was still above 90% and average error (NMAE) 20–21%. The 12-hour daytime AOT values could not be estimated with as high accuracy. The abilities of the methods to estimate 7-day AOT40 from average O_3 concentrations and measurement of air temperature variability are shown in Table 3 and in **Paper IV**.

Table 3. The ability of the Gaussian and trigonometric methods to estimate 7-day AOT40 from average O_3 concentrations and air temperature measurements. R^2 = coefficient of determination, ME = modelling efficiency and NMAE = normalized mean absolute error.

Method	Index	Linear regression	R^2	ME	NMAE
Gaussian	24-hour AOT40	y=0.92x+57	0.96	0.96	21%
Gaussian	12-hour AOT40	y=1.33x-15	0.89	0.61	44%
Trigonometric	24-hour AOT40	y=0.91x+26	0.95	0.95	20%
Trigonometric	12-hour AOT40	y=1.24x-2	0.92	0.77	40%

4.3 Local scale variation in stomatal O_3 uptake

Both average O_3 concentrations and DOR were found to differ considerably between the inland low, inland high and coastal sites. A relevant question in this context is if the relative risk of negative effects on vegetation due to O_3 exposure was different at the different site types. In addition to the O_3 concentrations in the ambient air, temperature,

humidity and irradiance also influence the uptake of O_3 through the plant stomata. Differences in local climate between sites could result in different risk of negative effects on vegetation.

Based on O_3 concentrations and meteorological condition measured with the mobile monitoring station the stomatal O_3 uptake was calculated. The generic crop (POD_{3crop}) parameterisation of the stomatal conductance model was used (**Paper III**). Since the mobile monitoring station was only placed one month at each site, data were not available to calculate the stomatal uptake of O_3 accumulated over the whole growing season (three months for POD_{3crop}). The calculated stomatal O_3 uptake from each of the different sites was compared to the reference site Östad. A consistent relationship between relative altitude (or altitude) and phytotoxic O_3 dose was not found for the one month periods (data not shown) at the inland sites. The light response function, which is largely an on-off function, was very similar between sites. According to the model parameterisation of POD_{3crop}, VPD was predicted to seldom limit the stomatal conductance at these sites (f_{VPD} seldom below 1), reflecting a relatively humid climate. The largest difference found between sites, besides the differences in O_3 concentrations, was in the temperature limitation of the stomatal conductance. At midday the average f_{temp} was less limiting at Östad, due to higher temperatures, compared to the other sites.

The calculated accumulated stomatal O_3 uptake was 28% larger at the coastal site Nidingen compared to Östad based on the 48 days of measurements. The difference was mainly attributed to the higher O_3 concentrations at Nidingen. At the other coastal site Rönnäng, only 8 rather cold days of complete measurements were available, which was not enough to show any difference in calculated stomatal O_3 uptake compared to Östad.

In **Paper V** the stomatal O_3 uptake of wheat and potato was calculated both based on measurements at Östad and based on EMEP model output from the 50×50 km^2 grid-cell in which Östad is situated. The EMEP model output correlated well with observed O_3 concentrations and meteorological conditions at Östad. Deviations between model and measurements were considerably larger during night-time than during day. However, it did not result in significant differences in calculated O_3 uptake. The calculated phytotoxic O_3 dose (POD_6) obtained using modelled or measured O_3 concentrations and meteorological conditions agreed rather well (within 10–20%).

4.4 O_3 risk for vegetation in the future climate of Europe

Future climate change has the potential to affect both the O_3 concentrations in the ambient air and the stomatal O_3 uptake. The resulting change in O_3 risk for vegetation was investigated in **Paper VI**. Figure 10 shows the average O_3 concentrations and AOT40 at ten EMEP sites based on modelled data from the corresponding grid-cell in the MATCH model in reference climate (1961–1990). The concentration-based O_3 risk for vegetation, estimated with the AOT40 index, follow the same geographical pattern as the O_3

concentrations, indicating largest risk in Southern Europe. The current critical levels are an AOT40 of 3 ppm h during three months for agricultural crops and 5 ppm h during the growing season for forests (LRTAP Convention, 2004). Exceedance of the critical level may cause reduced yield for agricultural crops and reduced growth for forest trees. As shown in Figure 10 the critical level for agricultural crops was exceeded at six out of ten monitoring stations whereas the forest critical level was exceeded at eight out of ten monitoring stations. Note however, that the growing seasons in this study are based on latitude and differs from the time periods used in e.g. EU directives for vegetation risk assessment.

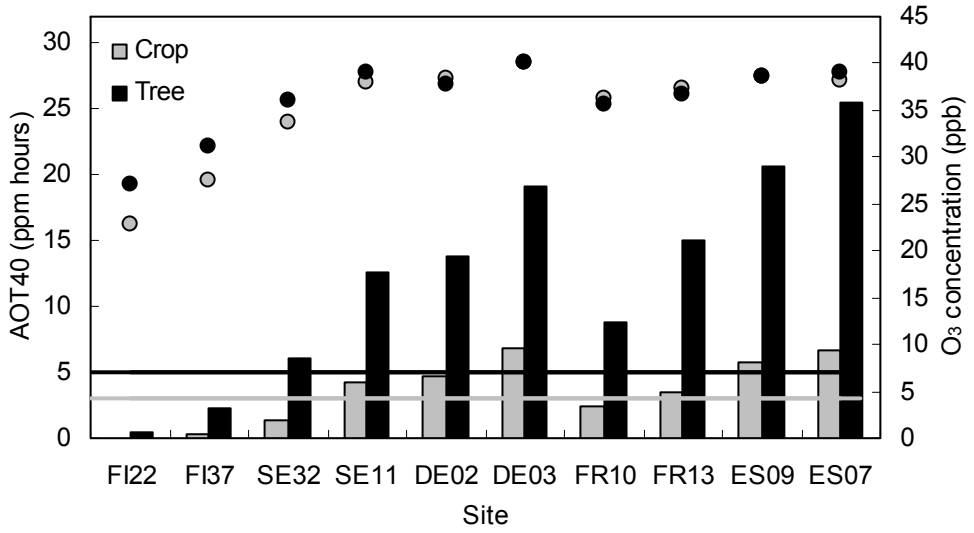

Figure 10. Average daylight AOT40 (bars, left y-axis) and average O_3 concentrations (circles, right y-axis) calculated for the generic crop and generic deciduous tree growing season based on modelled O_3 data from the MATCH model 1961–1990. Grey line is current critical level for crops (3 month time interval) and black line is current critical level for forests (April–September).

At six of the ten sites investigated, there is a large increase in future AOT40, especially in the 2071–2100 A2 emission scenario, where five sites (DE03, FR10, FR13, ES09 and ES07) will experience more than a doubling of AOT40. The four Nordic sites (FI22, FI37, SE32 and SE11) exhibit small changes in AOT40. Since anthropogenic emissions of O_3 precursors were held constant during the simulations, the increase in O_3 concentrations is entirely due to changes in the climate.

The geographical pattern of POD_{3crop} is considerably different compared to that of AOT40 (Figure 11). The stomatal O_3 flux is largest in Central Europe in both reference and future climate. The assumed reduction in stomatal conductance is 34% in the 2071–2100 A2 period due to CO_2 concentrations above 550 ppm. As a result, the sites with the largest increase in AOT40 by 2071–2100 in the A2 emission scenario show non-significant changes in POD_{3crop} (DE03 and FR10) or a large decrease in POD_{3crop} (statistically significant with $p<0.0001$ for FR13, ES09 and ES07). The two Swedish sites show a small but significant increase in POD_{3crop} ($p=0.012$ for SE32 and $p=0.027$ for SE11) during the same period.

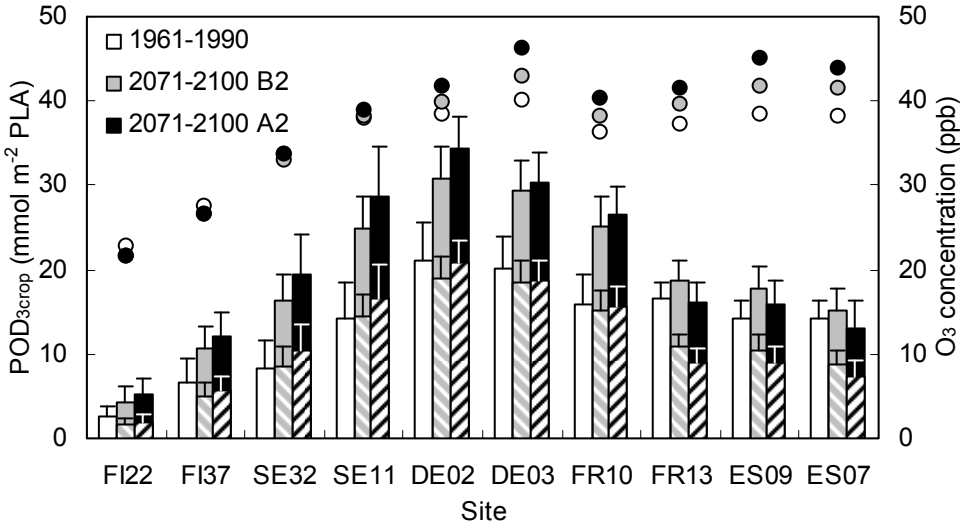

Figure 11. Average phytotoxic O_3 dose for a generic crop (POD_{3crop}) during reference climate (1961–1990), 2071–2100 following the SRES B2 emission scenario and 2071–2100 following the SRES A2 emission scenario (bars, left y-axis). The striped part of the bars show average POD_{3crop} when the stomatal conductance response function for CO_2 (f_{CO2}) is included in the calculation. Error bars show standard deviation (N=30 years). Circles are average O_3 concentrations (right y-axis) for the same time periods as POD_{3crop} is accumulated.

The O_3 concentrations are low and the temperature function significantly limits the stomatal conductance (average f_{temp} substantially below 1) at the northern sites. Without the inclusion of f_{CO2}, $POD3_{crop}$ increase significantly at the Nordic sites in the 2071–2100 A2 period compared to the reference period ($p<0.0001$ for FI22, FI37, SE32 and SE11). Higher temperatures and, for SE11, to some extent higher O_3 concentrations explain the increase. For example, without the influence of f_{CO2}, POD_{3crop} more than double at FI22 while the average O_3 concentration decrease by approximately 1 ppb. In Central Europe, the O_3 concentrations are high and climatic conditions favour stomatal O_3 uptake. When f_{CO2} is not included in the calculation, the large increase in O_3 concentrations by 2071–2100 A2, together with considerably higher f_{temp}, but only slightly lower f_{VPD} result in a significantly increased stomatal O_3 flux compared to reference climate ($p<0.0001$ for DE02, DE03 and FR10). At the three southernmost sites (FR13, ES09 and ES07) the stomatal conductance is, according to the model, substantially limited by f_{VPD} already in reference climate. Average f_{VPD} at the southernmost site (ES07) is for example 0.75 compared to 1.00 at the site with largest $POD3_{crop}$ (DE02). Despite a large increase in O_3 concentration (5 ppb on average) by 2071–2100 A2, the modelled stomatal O_3 flux does not increase in the future climate, due to increased VPD.

The general pattern in O_3 risk for vegetation is similar for the A2 and B2 emission scenarios. However, at the five southernmost sites the increase in O_3 concentration is smaller in the B2 emission scenario compared to A2 (2.7 ppb difference between 2071–2100 B2 and the reference period, compared to 5.3 ppb in A2). In addition, f_{VPD} does not limit the stomatal conductance at the southernmost sites to the same extent in the B2

emission scenario and the increase in stomatal conductance due to increasing temperature at the northernmost sites is not as large.

The geographical pattern of the generic deciduous tree $POD_{1.6tree}$ following the A2 scenario is similar to that for a generic crop (POD_{3crop}), with largest stomatal O_3 flux in Central Europe. Due to the assumed reduction of stomatal conductance by 20% with CO_2 concentrations above 550 ppm $POD_{1.6tree}$ was significantly reduced in the 2071–2100 A2 period compared to the reference period at all sites ($p<0.0001$).

When the influence of f_{CO2} is not included in the calculation, low and decreasing O_3 concentrations as well as low average f_{temp} result in small $POD_{1.6tree}$ at the two northernmost sites (FI22 and FI37), and no significant change by 2071–2100 A2. SE32, SE11 and DE02 experience increased stomatal O_3 flux in the 2071–2100 A2 period ($p<0.0001$) compared to the reference period, explained by increases in O_3 concentration and average f_{temp}. At the southernmost sites (FR13, ES09 and ES07) high temperatures limit the stomatal conductance in addition to the dry air conditions. It results in a significantly reduced stomatal O_3 flux ($p<0.0001$) despite a large increase in average O_3 concentrations. The inclusion of a SWP function in one $POD_{1.6tree}$ calculation indicated that f_{SWP} mainly limit O_3 uptake at the southern sites.

5. Discussion

5.1 Local climate and O_3 concentration variation

Even though ground-level O_3 is generally seen as a regional scale air pollutant, the results presented in this thesis clearly show that there is considerably local scale variation in O_3 concentrations. Two important sources of O_3 concentration variation in the landscape of south Sweden were identified (**Paper I, III**). Firstly, topography was found to be a very important factor explaining the diurnal dynamics of O_3 for inland sites. Inland low sites experienced stronger nocturnal temperature inversions, larger DOR and, due to the more marked nocturnal minima, lower average O_3 concentrations compared to inland high sites. Secondly, the coastal climate strongly influenced the O_3 concentrations and sites located in the vicinity of the coast experienced smaller DOR and higher average O_3 concentrations compared to inland sites, in agreement with other observations (e.g. Entwistle et al., 1997; Ribas and Peñuelas, 2004). Nocturnal temperature inversions, which in turn limit vertical O_3 transport, were found crucial in determining the differences in average O_3 concentrations and DOR between sites (**Paper III**). The nocturnal temperature inversions were weaker and the air mixing stronger at the inland high and coastal sites compared to the inland low sites. The importance of local meteorological conditions is emphasized by the similar diurnal variation in O_3 concentrations and air temperature between coastal and inland high sites, regardless of the different deposition velocities of O_3 over land and water (Galbally and Roy, 1980; Brook et al., 1999).

At the coastal sites advection of O_3-rich maritime air is also important for the enhanced O_3 concentrations. The vertical gradients of O_3 concentrations in the maritime boundary layer are small due to the low deposition velocity of O_3 over water. As this O_3-rich air crosses a coast and moves inland the larger deposition rates result in larger vertical gradients and a drop in O_3 concentrations near the surface (Entwistle et al., 1997). During on-shore wind directions the comparison of the off-shore island Nidingen and the coastal site Råö showed similar O_3 concentrations as both sites were influenced by the O_3-rich maritime air. During air flow from the inland the difference between the sites was larger, implying that the 6 km of open sea between the sites was sufficient to enhance the O_3 concentrations at Nidingen, while Råö was mostly influenced by inland air.

For purposes such as environmental monitoring it can be useful to relate average O_3 concentrations and DOR to DTR and topography, despite the large importance of

nocturnal temperature inversions. Measurements of DTR require less equipment (e.g. no mast) and topographical information for large areas (digital elevation maps) is also easier accessible compared to perform extensive measurements of the vertical temperature gradient. Relative altitude was superior to absolute altitude in explaining the landscape variation of average O_3 concentrations and DOR in south Sweden (**Paper III**). This was shown by e.g. the lower R^2 values using altitude compared to relative altitude. Relative altitude is more mechanistically relevant than altitude in explaining the diurnal dynamics of O_3 concentrations for inland sites. Local topography, as well as vicinity to the coast is therefore important to include when modelling O_3 concentrations in complex terrain.

The measurements with the mobile monitoring station represent different locations as well as different time periods (**Paper III, IV**). Spatial variation in O_3 concentrations and temperature is therefore confounded with temporal variation. However, different years and seasons (early, high, late summer) are well represented for the different site types. Thus, differences in O_3 concentrations and temperature dynamics among sites rather than among the measurement periods contribute to the relationships shown in Figure 5 and 7, **Paper III** and **Paper IV**. Furthermore, additional analyses of simultaneous O_3 concentration measurements were made in **Paper III**, which further supported the reliability of the results.

On a larger scale, the measurements performed at alpine Latnjajaure clearly indicated that this high-altitude site had higher O_3 concentrations than the permanent monitoring station Esrange, in the forested landscape below the mountain range (**Paper II**). A similar pattern, with higher O_3 at higher altitude, was also observed in northern Finland when Pallas (mountain) was compared with Oulanka (coniferous forest). It was explained by a smaller diurnal variation of O_3 at higher altitude and stronger coupling with the free troposphere, where the chemical lifetime of O_3 is longer (Rummukainen et al., 1996). The differences in the duration of the winter snow cover are probably also important.

5.2 Methodology to estimate AOT40 from average O_3

Based on measurements of O_3 concentrations and air temperature performed during the years 2005–2007 in the southwest of Sweden, it was shown that the diurnal ranges in O_3 concentrations and air temperature covariate (**Paper III, IV**), both temporally (at a specific site, days with a large DTR also have a large DOR) and spatially (sites with a large average DTR also have a large average DOR). The relationship between DOR and DTR can be used to estimate AOT40 from average O_3 concentrations in combination with air temperature measurements (**Paper IV**). This approach has now been applied for routine monitoring of O_3 risk for vegetation within the Ozone Monitoring Network in southern Sweden.

Both the Gaussian distribution method and the trigonometric method performed well in 24-hour AOT-estimations. Modelling efficiencies was higher the lower the threshold

concentration. Modelling efficiencies for 12-hour AOT-estimations were lower than for estimations of 24-hour AOT, indicating that the empirically derived parameters α and h_0 for different site types may be a too simple approach to estimate 12-hour AOT. If passive diffusion samplers could be exposed only during daytime, 12-hour AOT could be estimated with the same accuracy as 24-hour AOT (**Paper IV**). Equipment that would allow exposure of the passive diffusion samplers only during daytime are under development, but so far it has turned out to be difficult to apply for long-term, regular use (unpublished observations at the Swedish Environmental Research Institute).

5.3 The flux-based O_3 risk for vegetation

The O_3 concentration dynamics differed considerably between the inland low, inland high and coastal sites in southern Sweden, to a large part explained by differences in the local climate. Site specific environmental factors such as temperature, humidity and irradiance also influence the uptake of O_3 through the plant stomata. A relevant question in this context is if the relative risk of negative effects on vegetation due to O_3 exposure was different at the different site types.

A substantial difference in O_3 concentrations between inland and coastal sites during the day (e.g. between Råö and Östad in **Paper I** and between Nidingen and Östad in **Paper III**) imply an increased risk of negative effects on vegetation at coastal sites. The vegetation on the small island Nidingen is very sparse, but similar O_3 concentration patterns are likely to prevail at all sites in the vicinity of the coast, including those with sensitive vegetation.

Focusing on inland sites, relative altitude was not found to significantly influence the stomatal O_3 uptake (**Paper III**). However, the short measurement periods (approximately one month) and the limited number of parallel observations were found insufficient to determine to what extent relative altitude influences the risk of O_3 damage to vegetation. Only large differences between sites would be disclosed in the limited data set available. The insignificant difference in O_3 risk between inland low and inland high sites is also influenced by the choice to use the POD_{3crop} parameterisation of the stomatal conductance model. The use of a species-specific parameterisation with different sensitivity to e.g. VPD could change the result.

Relative altitude is mainly important in explaining differences in O_3 concentrations and temperature between inland high and low sites during night-time, due to the influence of topography on the formation of nocturnal temperature inversions (**Paper III**). Vegetation is most sensitive to the deleterious effects of O_3 during daytime, which is also when humans are mostly exposed. Many O_3 indices used to estimate O_3 risk for vegetation are not sensitive to nocturnal differences between sites. Relative altitude is therefore not necessarily as important in explaining differences in O_3 risk for vegetation between sites, as it is for average O_3 concentrations and DOR. However, nocturnal O_3 concentrations

cannot be completely neglected for plant O_3 uptake, in particular for trees (Uddling et al., 2004). In addition, differences in morning and evening O_3 concentrations can be of importance, especially at northern latitudes with a large number of daylight hours during summer and high O_3 concentrations extending far into the evening. Possible differences in stomatal O_3 uptake and O_3 risk for vegetation between sites due to relative altitude are probably small, but need further investigation.

The EMEP model and observations at Östad both gave similar estimates of O_3 uptake to plants, despite some differences in O_3 concentrations and meteorology (**Paper V**). The land-use in the EMEP grid-cell mainly consists of coniferous forest (73%) and differs substantially from the condition at the agricultural site Östad, situated in a broad valley with low vegetation. Despite the lower roughness characterising the Östad area compared to the surrounding forested landscape, the discrepancies between modelled and observed O_3 concentrations, temperature and VPD were only significant during night when the calculated uptake of O_3 by plants was limited by darkness.

Regional climate has a clear influence on the flux-based risk of O_3 damage to vegetation, as shown for Europe in **Paper VI**. The flux-based POD_Y index allows climatic conditions and the CO_2 concentrations to modify stomatal uptake rates of O_3, in line with important physiological processes and especially important in risk assessment of ground-level O_3 in a future with potential climate change. The AOT40 index only reflects changes in the ambient O_3 concentrations. In agreement with earlier studies (Simpson and Emberson, 2006; Emberson et al., 2007; Simpson et al., 2007), the spatial flux-based risk pattern for O_3 damage differed substantially from the AOT40-based risk in Europe (**Paper VI**).

Emberson et al. (2000b) found VPD to be the most important environmental factor limiting stomatal flux of O_3 in Europe. Based on the results in **Paper III, V, VI** the importance of f_{VPD} at the northern European sites appears to be restricted compared to the sites in Southern Europe. Instead temperature seems to be an important limiting factor, based on the current temperature functions for stomatal conductance in the UNECE Mapping Manual. The large importance of f_{temp} compared to f_{VPD} in limiting stomatal conductance in Northern Europe could be questioned, since minimizing water loss is a main function of the stomata. Furthermore, most physiological responses are known to acclimatize to the prevailing temperature (e.g. Larcher, 2003; Körner, 2006), indicating that both spatial (cold north vs. warm south) and temporal (during climate change) acclimation of the stomatal temperature response are likely. In a model simulation of O_3 flux for Norway spruce in northern Sweden, Karlsson et al. (2007b) found f_{VPD} to limit stomatal conductance to a greater extent at high compared to low O_3 concentrations. In O_3 concentrations above 40 ppb the stomatal conductance was limited approximately to the same extent by f_{VPD} and f_{temp}. It was explained by the association of high O_3 concentrations with sunny weather conditions, high air temperatures and high VPD. However, a certain degree of stomatal closure in response to low temperatures can be expected in colder conditions, due to the decrease in photosynthesis at cool, suboptimal temperatures. Further measurements and evaluation of the stomatal temperature response

function is required to improve the predictions of the effect of climate on stomatal O_3 flux.

5.4 O_3 risk and climate change

The strong and early (compared to southern Sweden) spring peak in O_3 was observed at all sites in northern Sweden, where year-round measurement was performed (**Paper II**). During summer the O_3 concentrations in the north were much lower than those observed in the south. A number of studies have shown an earlier onset of spring and a lengthening of the growing season in middle and high latitudes associated with global warming (Linderholm, 2006; Menzel et al., 2006), including northern Sweden (Karlsson et al., 2007b). At the present time the spring peak in northern Sweden occur before the start of the growing season, but an earlier onset of the growing season in future climate could result in an overlap. Karlsson et al. (2007b) showed that there is a substantial and increasing risk of negative impacts of O_3 on vegetation in northern Sweden, related mainly to increasing spring O_3 concentrations and an earlier onset of the growing season.

In agreement with the results of Harmens et al. (2007), the future flux-based risk of O_3 damage to vegetation was predicted to remain unchanged or decrease at most sites, despite substantially increased modelled O_3 concentrations in Central and Southern Europe. The expected reduction in stomatal conductance with rising atmospheric CO_2 concentrations is of large importance for this result. However, the magnitude of the CO_2 effect is uncertain, especially for trees, for which the long-term effects of elevated CO_2 concentrations on plant growth and stand structure may be more important than the primary stomatal closure response (Uddling et al., 2009). If the CO_2 effect will turn out to be small, many areas in Europe will experience an increasing risk of vegetation damage due to O_3 (**Paper VI**).

There are large uncertainties in both climate projections and parameters in models for O_3 risk assessment. O_3 uptake calculations may only be accurate when applied under conditions representative of those under which the parameterisation was performed since leaf properties determining the rate of O_3 uptake and the biochemical defence capacity can be modified by changes in temperature, air humidity, soil moisture and increasing CO_2 concentrations (Fuhrer, 2009). Notwithstanding the uncertainties, we believe that there is high confidence in the general pattern and directions of change in the presented results of how future climatic conditions will influence the O_3 risk for vegetation in Europe.

5.5 Concluding remarks

Climate has been shown to influence ground-level O_3 concentrations through a wide range of processes on different spatial and temporal scales. The results presented in this

thesis contribute to an increased understanding of the processes that cause local scale variation in O_3 exposure in Sweden. In particular, nocturnal temperature inversions which inhibit vertical mixing, advection of O_3-rich marine air, deposition rates to water, soil and vegetation, the duration of snow cover and local NO_x emission causing NO_x titration of O_3, are processes that result in significant local scale variations in O_3 concentrations. These processes strongly depend on meteorological conditions and are therefore highly sensitive to climate change.

Knowledge of the underlying processes causing local scale variation in O_3 concentrations is important. For purposes such as routine environmental monitoring the applicability under realistic conditions are just as important. The O_3 concentration variation was therefore related to site specific characteristics, such as site position in relation to the surrounding landscape and vicinity to the coast, resulting in different local climate. Previous studies have used altitude as such a dependence criterion of O_3 concentrations (e.g. Coyle et al., 2002), but the results presented in this thesis clearly show that topography, represented by relative altitude, is more mechanistically relevant than altitude in explaining the diurnal dynamics of O_3 for inland sites.

The variation in O_3 concentrations in the landscape of south-west Sweden mainly occurs during night-time. The degree of night-time O_3 depletion can be difficult to estimate, as reflected in e.g. the differences between modelled and observed night-time O_3 concentrations in **Paper V** and the difficulty in estimating 12-hour daytime AOT values in **Paper IV**. Since vegetation is most sensitive to the deleterious effects of O_3 during daytime, the use of long-term average O_3 concentrations and 24-hour AOT40 for risk assessment purposes should be viewed critically. Long-term average O_3 concentrations and 24-hour AOT40 are contaminated by nocturnal O_3 concentrations resulting in large deviations from the more relevant daytime concentrations at many locations, especially inland low sites.

Site specific meteorological conditions also influence the plant stomatal O_3 uptake. The flux-based approach (POD_Y-index) incorporates the modification of O_3 sensitivity by climatic conditions into the risk assessment. It is especially important to use the flux-based approach in assessing the future O_3 risk for vegetation, when potential climate change and elevated CO_2 concentrations need to be taken into account. With the exception of the study by Harmens et al. (2007), based on very simplified assumptions of the future climate, **Paper VI** is to my knowledge the first published study in which the flux-based approach has been used to assess the future O_3 risk for vegetation with consideration of climate change. Despite the uncertainties described in section 5.4, the use of the flux-based approach in this thesis is considered to be a large improvement compared to studies based on the still commonly used concentration-based approach (e.g. Van Dingenen et al., 2009 and Avnery et al., 2011).

6. Key findings

Ground-level O_3 concentrations vary on both a regional and local spatial scale. The differences in average O_3 concentrations, diurnal O_3 concentration range (DOR) and diurnal temperature range (DTR) between rural sites in southern Sweden are to a large degree explained by the strength of nocturnal temperature inversions. In addition, the underlying surface (important for the deposition rate), advection of O_3-rich marine air and local NO emissions were also important in determining the local scale variation of O_3 concentrations.

Average O_3 concentrations and DOR correlated with site position in the landscape in southern Sweden (high or low in relation to the surrounding terrain), represented by the relative altitude. Inland low sites experienced stronger nocturnal temperature inversions, larger DOR and lower average O_3 concentrations compared to inland high and coastal sites.

O_3 concentrations at the alpine site Latnjajaure, in the Scandian Mountain Range, were higher compared to the permanent monitoring station below the mountain range. The spring peak in O_3 was earlier and more pronounced at sites in northern compared to southern Sweden.

There is a correlation between DOR and DTR. This relationship makes it possible to estimate 24-hour AOT40 from average O_3 concentrations (measured with e.g. passive diffusion samplers) in combination with hourly air temperature measurements. The 12-hour daytime AOT40 values could not be estimated with as high accuracy. Complementing the permanent monitoring stations with the rather simple O_3 measurements based on passive diffusion samplers, result in a better geographical resolution of the AOT40–based risk for vegetation.

There is an increased flux-based risk of negative effects of O_3 on vegetation at coastal sites compared to inland sites mainly attributed to higher O_3 concentrations in the vicinity of the coast. However, significant differences in modelled stomatal O_3 uptake were not found between inland low and inland high sites. Hence, the fifth hypothesis was only partly corroborated.

A large part of the variation in O_3 concentrations at inland sites in south-west Sweden occurs during night-time. At night the stomatal O_3 uptake by vegetation is low and the risk of O_3 damage is therefore not greatly influenced. Thus, plant O_3 uptake and daytime

AOT40 are less influenced by the site position in the landscape than 24-hour average O_3 concentrations. The use of long-term average O_3 concentrations and 24-hour AOT40 for risk assessment purposes should be viewed critically since the inclusion of nocturnal O_3 concentrations result in geographical variation which is not reflected to the same extent in the more relevant daytime concentrations.

When evaluating regional scale models with measurements it is important to keep within grid variation and the representativeness of the measurement site in mind. The local site-specific differences are most pronounced in synoptic weather situations dominated by anti-cyclonic weather.

The future flux-based risk of O_3 damage to vegetation was predicted to remain unchanged or decrease in Europe, despite substantially increased modelled O_3 concentrations in Central and Southern Europe. The expected reduction in stomatal conductance with rising atmospheric CO_2 concentrations is of large importance for this result. However, the magnitude of the CO_2 effect is uncertain, especially for trees. If the CO_2 effect will turn out to be small, future climate change has the potential to dramatically increase the flux-based O_3 risk for vegetation in Northern and Central Europe.

7. Outlook

The pronounced, high and early peak in O_3 concentrations in northern compared to southern Sweden deserves further investigation. Actually, there is still no overarching consensus on the mechanisms that lead to the formation of a spring O_3 maximum. Understanding the appearance of the spring peak in O_3 and the mechanisms that lead to its formation therefore remains a fundamental issue that has implications for both policy (e.g. abatement strategies) and atmospheric science (Monks, 2000). Further analysis of the data presented in **Paper II** in relation to snow cover might contribute to the increased understanding of this phenomenon. In addition to low deposition velocity (Galbally and Roy, 1980), the high albedo of snow, not only for visible light, but also for the UV-A radiation promotes the photolysis of NO_2 and thus O_3 formation (Simpson et al., 2002; Schnell et al., 2009). The importance of this aspect depends on to what extent local photochemistry, in contrast to long-range transported pollutants, is responsible for the spring peak in O_3. Furthermore, the role of vegetation deserves investigation. An earlier onset of the growing season in the future could lead to a decrease in the O_3 spring peak, since vegetation with a large, physiologically active leaf area and substantial gas exchange, tends to reduce ground-level O_3 concentrations through increased deposition.

Mechanistic models of stomatal conductance do not yet exist due to the incomplete understanding of the complex physiological mechanisms of stomatal response to combinations of environmental parameters such as light, air temperature, VPD and SWP. In addition to the (semi-)empirical multiplicative algorithm used in this thesis (**Paper III, V, VI**) to predict stomatal conductance (and O_3 risk by the POD_Y-index) a semi-mechanistic type of model has also been developed (Büker et al., 2007). It is based on the evidence of a close relationship between stomatal conductance and net photosynthetic rate (A_n) and calculates stomatal conductance as a function of A_n, CO_2 concentrations and relative humidity at the leaf surface. Stomatal responses to CO_2, light and temperature are included in the A_n model and act synergistically in contrast to the multiplicative algorithm. Büker et al. (2007) compared the two types of algorithms with observed stomatal conductance for wheat, grapevine and birch. The performance of the algorithms was similar, but the higher input requirements of the photosynthesis-based algorithm, because of the need to model net photosynthesis, were noted. However, an urgent need to include the influence of CO_2 under climate change conditions could favour the photosynthesis-based approach in the future.

The O_3 risk for vegetation depends on exposure, leaf uptake and the plant's defence capacity (Fuhrer, 2009). O_3 risk can therefore not be claimed to be understood based solely on O_3 uptake, but is co-determined by the plant's sensitivity per unit of O_3 uptake, i.e. the plant ability to handle oxidative stress (Matyssek et al., 2008). Tausz et al. (2007) argue that since global change effects may modify the physiological susceptibility to O_3, a flux-concept weighted by defence capacity should be tested. Musselman et al. (2006) also emphasized the need to consider detoxification mechanisms in flux-based models, but noted the large uncertainty in quantifying the various defence mechanisms in plants. Tuzet et al. (2011) presented a new model of O_3 deposition and detoxification, which accounts for diurnal variability of detoxification processes. Simulations with the model point out the pool of ascorbate located in the mesophyll cell wall to play a significant role in the detoxification of O_3.

The flux-based approach to estimate O_3 risk was considered to be the currently best available method and more biologically relevant to explain O_3 damage to plants compared to the concentration-based approach. It is however clear that much future work is left in the development of more mechanistic O_3 risk assessment methodologies.

O_3 flux is not only important for risk assessment. The stomatal O_3 flux is one of the processes determining the gradient in O_3 concentration near the ground. O_3 concentrations at different heights will not be modelled correctly, without accurate estimation of stomatal O_3 flux in the overall mass balance calculation. In a CTM sensitivity study, Andersson and Engardt (2010) found that changes in dry deposition could explain up to 80% of the of the modelled ground-level O_3 change from 1961–1990 to 2071–2100. In **Paper VI** the canopy-scale O_3 dry deposition to vegetation in MATCH is a function of soil moisture, air humidity, temperature and irradiance. The stomatal flux of O_3 to the sunlit leaf level of specified vegetations types (POD_Y) was however calculated off-line. It means that the calculated O_3 uptake by vegetation does not affect the modelled ambient air O_3 concentrations in each time-step. It will most likely not affect the general pattern and directions of change in the calculated future O_3 risk for vegetation in Europe. However, an important way forward is to incorporate the stomatal O_3 flux calculations into the MATCH model and calculate the O_3 uptake by vegetation online.

O_3 is not only an issue for air quality. Based on direct radiative forcing tropospheric O_3 is ranked as the third most important greenhouse gas, after CO_2 and CH_4 (IPCC, 2007). Many processes and feedbacks come into play when considering the interactions between climate and O_3. For example, vegetation is an important carbon sink in the climate system, due to the uptake of CO_2 and carbon assimilation in plants. In a model study, Sitch et al. (2007) quantified the indirect effect whereby ground-level O_3 pollution can decrease the ability of plants to remove CO_2 from the atmosphere. Net photosynthesis was modified by a factor that accounts for plant O_3 uptake and plant-specific sensitivities to O_3 uptake. The result showed that the negative effects of O_3 on plant productivity have the potential to significantly suppress the global land-carbon sink. The CO_2-induced stomatal closure was found to offset the O_3 suppression of gross primary production by more than one third. It emphasises that the combined effects of climatic conditions and elevated CO_2

concentrations on future O_3 risk for vegetation are important for future crop and forest production and should be accounted for in coupled biosphere-climate models.

Ground-level O_3 has the potential to become a very serious threat to human health, food security and ecosystems later this century if insufficient control measures are implemented (The Royal Society, 2008). Major research gaps still remain in understanding basic processes and feedbacks between climate, O_3 concentration variation and ecosystems. This thesis adds a few pieces in the puzzle and, in the course of time, hopefully contributes to a better air quality and an improved environment.

Populärvetenskaplig sammanfattning

Marknära ozon (O_3) är en luftförorening som orsakar skördebortfall för grödor, minskad skogstillväxt och har negativa effekter på människors hälsa i stora delar av världen. O_3 bildas i luften när kväveoxider (NO_x) och flyktiga organiska kolväten (VOC) reagerar under inverkan av solljus. Eftersom mänskliga utsläpp av NO_x och VOC har ökat stort sedan industrialiseringen har även halten O_3 ökat. Idag räknas O_3 till ett av de allvarligaste luftföroreningsproblemen i stora delar av världen. Väderförhållanden och klimat påverkar hur hög halten av O_3 är på en rad olika sätt. Till exempel är den kemiska produktionen av O_3 i atmosfären störst under varmt och soligt väder och vindar kan transportera O_3 och O_3-bildande ämnen långa sträckor från områdena där utsläppen sker.

Marknära O_3 brukar ses som ett regionalt luftföroreningsproblem, där O_3-koncentrationen är ungefär densamma över ett större geografiskt område, som till exempel södra Sverige. Dock varierar O_3-koncentrationen också på lokal skala och kan skilja sig mellan platser på bara några kilometers avstånd. Det är viktigt att förstå hur stor den lokala variationen är och vilka som är de bakomliggande processerna för att kunna uppskatta risken för att människor och växter exponeras för skadliga nivåer av O_3. Jag har undersökt hur O_3-koncentrationen varierar i sydvästra Sverige och kopplat det till skillnader i det lokala klimatet mellan höglänta och låglänta platser i inlandet samt kustnära platser. O_3-koncentration och meteorologi mättes med en mobil mätstation som placerades ca en månad vardera på olika platser under sommaren 2005–2007. Dessutom mättes O_3 och NO_2-koncentrationen med passiva diffusionsprovtagare och O_3-data från permanenta miljöövervakningsstationer analyserades.

Vid kusten och högt belägna platser så var skillnaden mellan dag och natt både i temperatur och O_3-koncentration mindre och medelhalten av O_3 högre jämfört med lågt liggande platser. Skillnader mellan platser var störst på natten och kunde till stor del förklaras av nattliga inversioner. Vid en inversion ökar temperaturen i atmosfären med höjden, vilket leder till en stabil skiktning där kall luft (högre densitet, ”tung”) befinner sig under varm luft (lägre densitet, ”lättare”). Då dämpas alla vertikala luftrörelser. I sådana förhållanden kan O_3-koncentrationen i luftlagren närmast marken minska markant eftersom O_3 förbrukas genom att avsättas (deponeras) på markytan och vegetationen, men inget nytt O_3 tillförs från luftlager högre upp och ingen kemisk bildning av O_3 kan ske på natten. Inversioner inträffar framför allt klara och vindstilla nätter. De är vanligare och starkare på låglänta platser eftersom den kalla (”tunga”) luften ansamlas i dalgångar och svackor. Vid kusten påverkas också O_3-halten av att depositionen av O_3 mot vattenytor är mycket mindre än vad den är mot växter och mark.

Växter har små öppningar på bladen där gasutbytet med den omgivande luften sker, till exempel av koldioxid (CO_2), vattenånga (H_2O) och syre (O_2). Det är när O_3 kommer in i växten genom dessa så kallade klyvöppningar som det ställer till skada. Risken för O_3-skador på växter beror alltså inte bara på halten O_3 i den omgivande luften utan också på hur mycket O_3 som upptas genom klyvöppningarna. Växter kan reglera gasutbytet genom

att öppna och stänga klyvöppningarna, något som starkt påverkas av väderförhållanden och klimat. Till exempel stängs klyvöppningarna när det är torrt för att växten inte ska förlora vatten genom avdunstning. Med hjälp av modeller kan O_3-upptaget genom klyvöppningarna beräknas utifrån O_3-koncentrationen i den omgivande luften och meteorologiska faktorer som temperatur, luftfuktighet och solljus. Därigenom uppskattas risken för att O_3 ska skada växterna.

I sydvästra Sverige tyder beräkningarna på att det är inte är någon större skillnad i risk för O_3-skador på växterna mellan höglänta och låglänta platser i inlandet. Det beror på att skillnaden i O_3-koncentration mellan höglänta och låglänta platser är störst på natten, men ungefär lika över ett större område under dagen. På natten är upptaget av O_3 genom klyvöppningarna litet eftersom de stängs när det är mörkt och ingen fotosyntes kan ske. Däremot leder höga O_3-koncentrationer vid kusten till att det där är högre risk för O_3-skador på växterna.

De senaste 100 åren har den globala medeltemperaturen ökat med 0.74 °C. Jordens klimat håller på att förändras, till stor del på grund av mänskliga utsläpp av växthusgaser. Samtidigt har jordens befolkning ökat kraftigt och efterfrågan på naturresurser och mat ökar. Mot den bakgrunden är det viktigt att förstå hur risken för O_3-skador på jordbruksgrödor och träd kommer att förändras i ett förändrat klimat. Jag har uppskattat risken för O_3-skador i Europa genom att beräkna upptaget av O_3 genom klyvöppningarna baserat på O_3-koncentrationer från en atmosfärskemimodell (MATCH) och meteorologi från en regional klimatmodell (RCA3). Beräkningarna har gjorts för två framtida globala scenarion för hur utsläppen av växthusgaser förändras (IPCC SRES scenario A2 och B2). Mänskliga utsläpp av ozonbildande ämnen (NO_x och VOC) var desamma som dagens i modellen för att hålla isär effekten av ändrat klimat och ändrade utsläpp.

Både i nuvarande och framtida klimat är risken för O_3-skador störst i centrala Europa. Där är O_3-koncentrationen hög och klimatförhållandena främjar växternas upptag av O_3 genom klyvöppningarna. I norra Europa är risken jämförelsevis liten, dels för att O_3-koncentrationerna är låga och dels för att växternas upptag av O_3 enligt modellen är begränsat av låga temperaturer. I södra Europa är O_3-koncentrationerna höga, men torka begränsar enligt modellen kraftigt växternas upptag av O_3.

Enligt modellberäkningarna kommer risken för O_3-skador på grödor och lövträd att vara densamma eller minska under i framtiden (2071–2100) jämfört med dagens klimat. Det beror framför allt på antagandet att växternas klyvöppningar är mindre öppna när koncentrationen av CO_2 i atmosfären ökar. Växterna kan då ta upp samma mängd CO_2, men förlora mindre vatten. Det är osäkert hur stor den effekten kommer att bli, speciellt för träd. Om det visar sig att CO_2-effekten på klyvöppningarna blir liten så har det framtida klimatet i norra och centrala Europa potential att kraftigt öka risken för O_3-skador i slutet av detta århundrade. I södra Europa ändras inte risken trots ökade O_3-halter eftersom mycket torra förhållanden förväntas kraftigt begränsa växternas O_3-upptag genom klyvöppningarna i framtida klimat.

Acknowledgements

It was possible to complete this thesis thanks to many people to whom I would like to express my gratitude. First of all I want to thank Håkan Pleijel, who I believe is the best supervisor any PhD-student could wish for. I also owe many thanks to my assistant supervisors Per Erik Karlsson and Deliang Chen, for sharing knowledge and experience of measurements as well as for good advice, encouragement and new angles of approach. In addition to my supervisors, I have been privileged to work with a number of nice, competent and helpful people. I especially want to acknowledge my co-authors Helena Danielsson, Magnuz Engardt, Gunilla Pihl Karlsson, Kristin Piikki, David Simpson, Johan Uddling, Mats Björkman and Yumei Hu.

Per Erik Karlsson, Gunilla Pihl Karlsson and I have shared a few adventures travelling around south Sweden with the mobile monitoring station in sunshine and in rain, not to mention fog. The kind treatment and practical support from the people we met in connection with the location of the mobile monitoring station has been invaluable. I also wish to thank Ann Parinder, Lena Eriksson and their families, who let me put up equipment and measure air pollutants in their gardens in Gothenburg.

At the Department of Plant and Environmental Sciences I have been surrounded and supported by so many terrific colleagues I hope you forgive me for not mentioning you all by name. Thanks for everything from indescribably amusing fika-discussions to practical help to “get along” with my computer. Special thanks to my previous and present office room mates Delilah Lithner, Lasse Tarvainen and Erik Heyman for encouragement, inspiration, relieving grumbling-sessions (usually about EXCEL) and valuable tips ranging from bread-baking to the lay-out of a thesis.

My PhD project has been part of the multidisciplinary Graduate School Climate and Mobility, which has added both very interesting interdisciplinary discussions and new friends to my life. Part of my PhD project was performed within the MISTRA-funded research programme ASTA (International and National Abatement Strategies for Transboundary Air Pollution) and the research programme CLEO (Climate Change and Environmental Objectives) funded by the Swedish Environmental Protection Agency. Financial support for measurements and trips to conferences and courses has gratefully been received from Filosofiska fakulteternas gemensamma donationsnämnd, Wilhelm och Martina Lundgrens Vetenskapsfond 1, Helge Ax:son Johnsons stiftelse, Adlerbertska forskningsstiftelsen, Ångpanneföreningens Forksningsstiftelse, the County Administration Boards of Västra Götaland, Halland and Skåne, the Swedish Environmental Protection Agency and the Graduate School Climate and Mobility.

Last but certainly not least: My friends - many thanks and lots of hugs for support, distraction and fun, in good times and in bad. My family - thanks for loving me, believing in me, always being there for me and lately for a whole lot of baby-sitting... Most important of all; my husband Markus and our son Thomas - thanks for reminding me of what is important in life when I’m lost and for making me laugh when I need it the most!

References

Ainsworth, E. A. and Rogers, A. 2007. The response of photosynthesis and stomatal conductance to rising [CO_2]: mechanisms and environmental interactions. *Plant Cell and Environment* **30**, 258-270.

Andersson, C. and Engardt, M. 2010. European ozone in a future climate: Importance of changes in dry deposition and isoprene emissions. *Journal of Geophysical Research-Atmospheres* **115**, D02303. doi:02310.01029/02008JD011690.

Ashmore, M. R. 2005. Assessing the future global impacts of ozone on vegetation. *Plant, Cell & Environment* **28**, 949-964.

Avnery, S., Mauzerall, D. L., Liu, J. and Horowitz, L. W. 2011. Global crop yield reductions due to surface ozone exposure: 2. Year 2030 potential crop production losses and economic damage under two scenarios of O_3 pollution. *Atmospheric Environment* **45**, 2297-2309.

Ayers, G. P., Keywood, M. D., Gillett, R., Manins, P. C., Malfroy, H. and Bardsley, T. 1998. Validation of passive diffusion samplers for SO_2 and NO_2. *Atmospheric Environment* **32**, 3587-3592.

Bazhanov, V. and Rodhe, H. 1997. Tropospheric ozone at the Swedish mountain site Åreskutan: budget and trends. *Journal of Atmospheric Chemistry* **28**, 61-76.

Berge, E. and Jakobsen, H. A. 1998. A regional scale multilayer model for the calculation of long-term transport and deposition of air pollution in Europe. *Tellus B* **50**, 205-223.

Brook, J. R., Zhang, L., Li, Y. and Johnson, D. 1999. Description and evaluation of a model of deposition velocities for routine estimates of dry deposition over North America. Part II: review of past measurements and model results. *Atmospheric Environment* **33**, 5053-5070.

Büker, P., Emberson, L. D., Ashmore, M. R., Cambridge, H. M., Jacobs, C. M. J., Massman, W. J. *et al.* 2007. Comparison of different stomatal conductance algorithms for ozone flux modelling. *Environmental Pollution* **146**, 726-735.

Carmichael, G. R., Ferm, M., Thongboonchoo, N., Woo, J. H., Chan, L. Y., Murano, K. *et al.* 2003. Measurements of sulfur dioxide, ozone and ammonia concentrations in Asia, Africa, and South America using passive samplers. *Atmospheric Environment* **37**, 1293-1308.

Coyle, M., Smith, R. I., Stedman, J. R., Weston, K. J. and Fowler, D. 2002. Quantifying the spatial distribution of surface ozone concentration in the UK. *Atmospheric Environment* **36**, 1013-1024.

Dentener, F., Stevenson, D., Ellingsen, K., van Noije, T., Schultz, M., Amann, M. *et al.* 2006. The global atmospheric environment for the next generation. *Environmental Science & Technology* **40**, 3586-3594.

Derwent, R. G., Stevenson, D. S., Collins, W. J. and Johnson, C. E. 2004. Intercontinental transport and the origins of the ozone observed at surface sites in Europe. *Atmospheric Environment* **38**, 1891-1901.

Diem, J. E. 2003. A critical examination of ozone mapping from a spatial-scale perspective. *Environmental Pollution* **125**, 369-383.

Emberson, L., Simpson, D., Tuovinen, J. P., Ashmore, M. and Cambridge, H. M. 2000a. Towards a model of ozone deposition and stomatal uptake over Europe. EMEP MSC-W Note 6/2000. Norwegian Meteorological Institute, Oslo, Norway. Available at www.emep.int.

Emberson, L. D., Ashmore, M. R., Cambridge, H. M., Simpson, D. and Tuovinen, J. P. 2000b. Modelling stomatal ozone flux across Europe. *Environmental Pollution* **109**, 403-413.

Emberson, L. D., Ashmore, M. R., Murray, F., Kuylenstierna, J. C. I., Percy, K. E., Izuta, T. *et al.* 2001. Impacts of Air Pollutants on Vegetation in Developing Countries. *Water, Air, and Soil Pollution* **130**, 107-118.

Emberson, L. D., Büker, P. and Ashmore, M. R. 2007. Assessing the risk caused by ground level ozone to European forest trees: A case study in pine, beech and oak across different climate regions. *Environmental Pollution* **147**, 454-466.

Entwistle, J., Weston, K., Singles, R. and Burgess, R. 1997. The magnitude and extent of elevated ozone concentrations around the coasts of the British Isles. *Atmospheric Environment* **31**, 1925-1932.

Fagerli, H., Simpson, D. and Tsyro, S. 2004. Unified EMEP model: Updates, p 11-18 in EMEP Status Report 1/2004, Norwegian Meteorological Institute, Oslo, Norway. Available at www.emep.int.

Ferm, M. 2001. Validation of a diffusive sampler for ozone in workplace atmospheres according to EN838. In: Proceedings of the International conference on measuring air pollutants by diffusive sampling, Montpellier, France, 26-28 September, 2001.

Ferm, M. and Rodhe, H. 1997. Measurements of Air Concentrations of SO_2, NO_2 and NH_3 at Rural and Remote Sites in Asia. *Journal of Atmospheric Chemistry* **27**, 17-29.

Ferm, M. and Svanberg, P.-A. 1998. Cost-efficient techniques for urban- and background measurements of SO_2 and NO_2. *Atmospheric Environment* **32**, 1377-1381.

Fowler, D., Pilegaard, K., Sutton, M. A., Ambus, P., Raivonen, M., Duyzer, J. *et al.* 2009. Atmospheric composition change: Ecosystems-Atmosphere interactions. *Atmospheric Environment* **43**, 5193-5267.

Fuhrer, J. 2009. Ozone risk for crops and pastures in present and future climates. *Naturwissenschaften* **96**, 173-194.

Galbally, I. E. and Roy, C. R. 1980. Destruction of ozone at the earth's surface. *Quarterly Journal of the Royal Meteorological Society* **106**, 599-620.

Garland, J. A. and Derwent, R. G. 1979. Destruction at the ground and the diurnal cycle of concentration of ozone and other gases. *Quarterly Journal of the Royal Meteorological Society* **105**, 169-183.

Geiger, R., Aron, R. H. and Todhunter, P. 2003. *The climate near the ground, 6th edition*. Rowman and Littlefield Publishers, Inc, USA.

Gerosa, G., Ferretti, M., Bussotti, F. and Rocchini, D. 2007. Estimates of ozone AOT40 from passive sampling in forest sites in South-Western Europe. *Environmental Pollution* **145**, 629-635.

Gibson, M. D., Guernsey, J. R., Beauchamp, S., Waugh, D., Heal, M. R., Brook, J. R. *et al.* 2009. Quantifying the spatial and temporal variation of ground-level ozone in the rural Annapolis Valley, Nova Scotia, Canada using nitrite-impregnated passive samplers. *Journal of the Air & Waste Management Association* **59**, 310-320.

Gilbert, N. L., Woodhouse, S., Stieb, D. M. and Brook, J. R. 2003. Ambient nitrogen dioxide and distance from a major highway. *The Science of the Total Environment* **312**, 43-46.

Gottardini, E., Cristofori, A., Cristofolini, F. and Ferretti, M. 2010. Variability of ozone concentration in a mountain environment, northern Italy. *Atmospheric Environment* **44**, 147-152.

Hall, D. G. M., Reeve, M. J., Thomson, A. J. and Wright, V. F. 1977. Water retention, porosity and density of field soils. Technical Monograph No 9. Soil Survey, Rothhamstead Experimental Station, UK.

Harmens, H., Mills, G., Emberson, L. D. and Ashmore, M. R. 2007. Implications of climate change for the stomatal flux of ozone: A case study for winter wheat. *Environmental Pollution* **146**, 763-770.

Hatakka, J., Aalto, T., Aaltonen, V., Aurela, M., Hakola, H., Komppula, M. *et al.* 2003. Overview of the atmospheric research activities and results at Pallas GAW station. *Boreal Environment Research* **8**, 365-383.

IPCC 2007. Solomon, S., D. Qin, M. Manning, Z. Chen, M. Marquis, K.B. Averyt, M. Tignor and H.L. Miller (eds.). *Climate change 2007: the physical science basis. Contribution of Working Group I to the Fourth Assessment Report of the Intergovernmental Panel on Climate Change*, Cambridge University Press, Cambridge, United Kingdom and New York, USA

Jacob, D. J. 1999. *Introduction to atmospheric chemistry*, Princeton University Press, UK.

Jacob, D. J. and Winner, D. A. 2009. Effect of climate change on air quality. *Atmospheric Environment* **43**, 51-63.

Janssen, P. H. M. and Heuberger, P. S. C. 1995. Calibration of process-oriented models. *Ecological Modelling* **83**, 55-66.

Jarvis, P. G. 1976. The interpretation of the variations in leaf water potential and stomatal conductance found in canopies in the field. *Philosophical Transactions of the Royal Society, London B* **87**, 593-610.

Jones, C. G., Samuelsson, P. and Kjellström, E. 2011. Regional climate modelling at the Rossby Centre. *Tellus A* **63**, 1-3.

Jones, H. G. 1992. *Plants and microclimate. A quantitative approach to environmental plant physiology, 2nd edition*. Cambridge University Press, UK.

Karlsson, P. E., Braun, S., Broadmeadow, M., Elvira, S., Emberson, L., Gimeno, B. S. *et al.* 2007a. Risk assessments for forest trees: The performance of the ozone flux versus the AOT concepts. *Environmental Pollution* **146**, 608-616.

Karlsson, P. E., Tang, L., Sundberg, J., Chen, D., Lindskog, A. and Pleijel, H. 2007b. Increasing risk for negative ozone impacts on vegetation in northern Sweden. *Environmental Pollution* **150**, 96-106.

Kjellström, E., Bärring, L., Gollvik, S., Hansson, U., Jones, C., Samuelsson, P. *et al.* 2005. A 140-year simulation of European climate with the new version of the Rossby Centre regional atmospheric climate model (RCA3). In: SMHI Reports Meteorology and Climatology No. 108, SMHI, SE-60176 Norrköping, Sweden, 54.

Körner, C. 2006. Significance of temperature in plant life. In: *Plant growth and climate change* (ed. Morison, J. I. L. and Morecraft, M. D.), Blackwell Publishing, Oxford, UK, 48-69.

Larcher, W. 2003. *Physiological Plant Ecology, 4th edition*. Springer-Verlag, Berlin, Germany.

Laurila, T. 1999. Observational study of transport and photochemical formation of ozone over northern Europe. *Journal of Geophysical Research D: Atmospheres* **104**, 26235-26243.

Laurila, T. and Hakola, H. 1996. Seasonal cycle of C_2-C_5 hydrocarbons over the Baltic Sea and Northern Finland. *Atmospheric Environment* **30**, 1597-1607.

Linderholm, H. W. 2006. Growing season changes in the last century. *Agricultural and Forest Meteorology* **137**, 1-14.

Lindkvist, L. and Lindqvist, S. 1997. Spatial and temporal variability of nocturnal summer frost in elevated complex terrain. *Agricultural and Forest Meteorology* **87**, 139-153.

Loibl, W., Winiwarter, W., Kopsca, A., Zueger, J. and Baumann, R. 1994. Estimating the spatial distribution of ozone concentrations in complex terrain. *Atmospheric Environment* **28**, 2557-2566.

LRTAP Convention 2004 (updated 2010). Manual on methodologies and criteria for modelling and mapping critical loads & levels and air pollution effects, risks and trends. Available and continuously updated at www.icpmapping.org.

Matyssek, R., Sandermann, H., Wieser, G., Booker, F., Cieslik, S., Musselman, R. *et al.* 2008. The challenge of making ozone risk assessment for forest trees more mechanistic. *Environmental Pollution* **156**, 567-582.

Meleux, F., Solmon, F. and Giorgi, F. 2007. Increase in summer European ozone amounts due to climate change. *Atmospheric Environment* **41**, 7577-7587.

Menzel, A., Sparks, T. H., Estrella, N., Koch, E., Aaasa, A., Ahas, R. *et al.* 2006. European phenological response to climate change matches the warming pattern. *Global Change Biology* **12**, 1969-1976.

Mills, G., Hayes, F., Simpson, D., Emberson, L., Norris, D., Harmens, H. *et al.* 2011. Evidence of widespread effects of ozone on crops and (semi-)natural vegetation in Europe (1990-2006) in relation to AOT40-and flux-based risk maps. *Global Change Biology* **17**, 592-613.

Monks, P. S. 2000. A review of the observations and origins of the spring ozone maximum. *Atmospheric Environment* **34**, 3545-3561.

Monteith, J. and Unsworth, M. H. 2008. *Principles of environmental physics, 3rd edition*. Academic Press, UK.

Musselman, R. C., Lefohn, A. S., Massman, W. J. and Heath, R. L. 2006. A critical review and analysis of the use of exposure- and flux-based ozone indices for predicting vegetation effects. *Atmospheric Environment* **40**, 1869-1888.

Nakicenovic, N., Alcamo, J., Davis, G., Vries, B. d., Fenhann, J., Gaffin, S. *et al.* 2000. *Emission scenarios. A special report of IPCC Working Group III*. Cambridge University Press, Cambridge, UK.

Oke, T. R. 1987. *Boundary Layer Climates, 2nd edition*. Routledge, UK.

Paoletti, E. and Manning, W. J. 2007. Toward a biologically significant and usable standard for ozone that will also protect plants. *Environmental Pollution* **150**, 85-95.

Pleijel, H., Danielsson, H., Emberson, L., Ashmore, M. R. and Mills, G. 2007. Ozone risk assessment for agricultural crops in Europe: Further development of stomatal flux and flux-response relationships for European wheat and potato. *Atmospheric Environment* **41**, 3002-3040.

Pleijel, H., Danielsson, H., Ojanperä, K., De Temmerman, L., Högy, P., Badiani, M. *et al.* 2004. Relationships between ozone exposure and yield loss in European wheat and potato - a comparison of concentration- and flux-based exposure indices. *Atmospheric Environment* **38**, 2259-2269.

Pleijel, H., Klingberg, J. and Bäck, E. 2009. Characteristics of NO_2 pollution in the City of Gothenburg, south-west Sweden - Relation to NO_x and O_3 levels, photochemistry and monitoring location. *Water, Air, & Soil Pollution: Focus* **9**, 15-25.

Prather, M., Gauss, M., Berntsen, T., Isaksen, I., Sundet, J., Bey, I. *et al.* 2003. Fresh air in the 21st century? *Geophysical Research Letters* **30**, 72-71 - 72-74.

Ribas, A. and Peñuelas, J. 2006. Surface ozone mixing ratio increase with altitude in a transect in the Catalan Pyrenees. *Atmospheric Environment* **40**, 7308-7315.

Ribas, À. and Peñuelas, J. 2004. Temporal patterns of surface ozone levels in different habitats of the North Western Mediterranean basin. *Atmospheric Environment* **38**, 985-992.

Robertson, L., Langner, J. and Engardt, M. 1999. An Eulerian limited-area atmospheric transport model. *Journal of Applied Meteorology* **38**, 190-210.

Rummukainen, M., Laurila, T. and Kivi, R. 1996. Yearly cycle of lower tropospheric ozone at the arctic circle. *Atmospheric Environment* **30**, 1875-1885.

Sanz, M. J., Calatayud, V. and Sánchez-Peña, G. 2007. Measures of ozone concentrations using passive sampling in forests of South Western Europe. *Environmental Pollution* **145**, 620-628.

Schnell, R. C., Oltmans, S. J., Neely, R. R., Endres, M. S., Molenar, J. V. and White, A. B. 2009. Rapid photochemical production of ozone at high concentrations in a rural site during winter. *Nature Geoscience* **2**, 120-122.

Seinfeld, J. H. and Pandis, S. N. 2006. *Atmospheric chemistry and physics: From air pollution to climate change, 2nd edition*. John Wiley & Sons, Inc., USA.

Sillman, S. 1999. The relation between ozone, NO_x and hydrocarbons in urban and polluted rural environments. *Atmospheric Environment* **33**, 1821-1845.

Simpson, D., Ashmore, M. R., Emberson, L. and Tuovinen, J. P. 2007. A comparison of two different approaches for mapping potential ozone damage to vegetation. A model study. *Environmental Pollution* **146**, 715-725.

Simpson, D. and Emberson, L. 2006. Ozone fluxes - updates, chapter 5 in EMEP status report 1/2006, Transboundary acidification, eutrophication and ground level ozone in Europe since 1990 to 2004. Available at www.emep.int.

Simpson, D., Fagerli, H., Jonson, J. E., Tsyro, S., Wind, P. and Tuovinen, J.-P. 2003a. Transboundary Acidification, Eutrophication and Ground Level Ozone in Europe. Part I. Unified EMEP Model Description. EMEP Status Report 2003. Norwegian Meteorological Institue, Oslo, Norway. ISSN 0806-4520. Available at www.emep.int.

Simpson, D., Tuovinen, J. P., Emberson, L. and Ashmore, M. R. 2001. Characteristics of an ozone deposition module. *Water, Air, & Soil Pollution: Focus* **1**, 253-262.

Simpson, D., Tuovinen, J. P., Emberson, L. and Ashmore, M. R. 2003b. Characteristics of an ozone deposition module II: Sensitivity analysis. *Water, Air, and Soil Pollution* **143**, 123-137.

Simpson, W. R., King, M. D., Beine, H. J., Honrath, R. E. and Peterson, M. C. 2002. Atmospheric photolysis rate coefficients during the Polar Sunrise Experiment ALERT2000. *Atmospheric Environment* **36**, 2471-2480.

Sitch, S., Cox, P. M., Collins, W. J. and Huntingford, C. 2007. Indirect radiative forcing of climate change through ozone effects on the land-carbon sink. *Nature* **448**, 791-794.

Sjöberg, K., Lövblad, G., Ferm, M., Ulrich, E., Cecchini, S. and Dalstein, L. 2001. Ozone measurements at forest plots using diffusive samplers. In: Proceedings of the International Conference Measuring Air Pollutants by Diffusive Sampling, Montpellier, France 26-28 September, 2001.

Solberg, S., Bergström, R., Langner, J., Laurila, T. and Lindskog, A. 2005a. Changes in Nordic surface ozone episodes due to European emission reductions in the 1990s. *Atmospheric Environment* **39**, 179-192.

Solberg, S., Derwent, R. G., Hov, O., Langner, J. and Lindskog, A. 2005b. European abatement of surface ozone in a global perspective. *Ambio* **34**, 47-53.

Stevenson, D. S., Dentener, F. J., Schultz, M. G., Ellingsen, K., van Noije, T. P. C., Wild, O. *et al.* 2006. Multimodel ensemble simulations of present-day and near-future tropospheric ozone. *Journal of Geophysical Research-Atmospheres* **111**, D08301. doi:10.1029/2005JD006338.

Stevenson, K., Bush, T. and Mooney, D. 2001. Five years of nitrogen dioxide measurement with diffusion tube samplers at over 1000 sites in the UK. *Atmospheric Environment* **35**, 281-287.

Svanberg, P.-A., Grennfelt, P. and Lindskog, A. 1998. The Swedish Urban Air Quality Network--A cost efficient long-term program. *Atmospheric Environment* **32**, 1407-1418.

Tabony, R. C. 1985. Relations between minimum temperature and topography in Great Britain. *Journal of Climatology* **5**, 503-520.

Tausz, M., Grulke, N. E. and Wieser, G. 2007. Defense and avoidance of ozone under global change. *Environmental Pollution* **147**, 525-531.

The Royal Society 2008. *Ground-level ozone in the 21st century: future trends, impacts and policy implications*. RS Policy document 15/08, London. Available at http://royalsociety.org.

Tilmes, S. and Zimmermann, J. 1998. Investigation on the spatial scales of the variability in measured near-ground ozone mixing ratios. *Geophysical Research Letters* **25**, 3827-3830.

Tuovinen, J.-P. 2002. Assessing vegetation exposure to ozone: is it possible to estimate AOT40 by passive sampling? *Environmental Pollution* **119**, 203-214.

Tuovinen, J. P., Simpson, D., Emberson, L., Ashmore, M. and Gerosa, G. 2007. Robustness of modelled ozone exposures and doses. *Environmental Pollution* **146**, 578-586.

Tuzet, A., Perrier, A., Loubet, B. and Cellier, P. 2011. Modelling ozone deposition fluxes: The relative roles of deposition and detoxification processes. *Agricultural and Forest Meteorology* **151**, 480-492.

Uddling, J., Pleijel, H. and Karlsson, P. E. 2004. Measuring and modelling leaf diffusive conductance in juvenile silver birch, Betula pendula. *Trees - Structure and Function* **18**, 686-695.

Uddling, J., Teclaw, R. M., Kubiske, M. E., Pregitzer, K. S. and Ellsworth, D. S. 2008. Sap flux in pure aspen and mixed aspen-birch forests exposed to elevated concentrations of carbon dioxide and ozone. *Tree Physiology* **28**, 1231-1243.

Uddling, J., Teclaw, R. M., Pregitzer, K. S. and Ellsworth, D. S. 2009. Leaf and canopy conductance in aspen and aspen-birch forests under free-air enrichment of carbon dioxide and ozone. *Tree Physiology* **29**, 1367-1380.

Van Dingenen, R., Dentener, F. J., Raes, F., Krol, M. C., Emberson, L. and Cofala, J. 2009. The global impact of ozone on agricultural crop yields under current and future air quality legislation. *Atmospheric Environment* **43**, 604-618.

Vardoulakis, S., Lumbreras, J. and Solazzo, E. 2009. Comparative evaluation of nitrogen oxides and ozone passive diffusion tubes for exposure studies. *Atmospheric Environment* **43**, 2509-2517.

Vingarzan, R. 2004. A review of surface ozone background levels and trends. *Atmospheric Environment* **38**, 3431-3442.

Volz, A. and Kley, D. 1988. Evaluation of the Montsouris series of ozone measurements made in the nineteenth century. *Nature* **332**, 240-242.

Yu, C. H., Morandi, M. T. and Weisel, C. P. 2008. Passive dosimeters for nitrogen dioxide in personal/indoor air sampling: A review. *Journal of Exposure Science and Environmental Epidemiology* **18**, 441-451.

Appendix – Calculation methods

1. The concentration-based O_3 index AOT40

AOTX is the sum of the difference between the hourly mean O_3 concentration at the top of the canopy ($C(z)$) and the threshold concentration X ppb for all daylight hours within a specified time period (unit: ppb hours):

$$AOTX = \int \max(C(z) - X, 0)dt \qquad \text{(Eq. 1)}$$

The time period for which AOTX is calculated should be three months for agricultural crops and the timing should reflect the period of active growth. The AOT40 index is used within the EU directive (2008/50/EC) on *Ambient Air Quality and Cleaner Air for Europe*, which is implemented in the Swedish legislation with the *Ordinance on Environmental Quality Standards for Ambient Air* (SFS 2010:477). In order to protect vegetation AOT40 should be strived not to exceed 9000 ppb hours as a five-year average. From 2020 and forward an AOT40 above 3000 ppb hours should be endeavoured not to occur in ambient air. Within the Swedish legislation, AOT40 is calculated during the period 1 May to 31 July and for daily hours 8–20. In the example shown in Figure A1, AOT40 is calculated for 19–20 June 2000, two days with high O_3 concentrations, at the reference site Östad. Only hours between 8 and 20 o'clock and when the O_3 concentration exceeds 40 ppb contribute to AOT40. In this particular case the AOT40 was calculated to be 434 ppb hours.

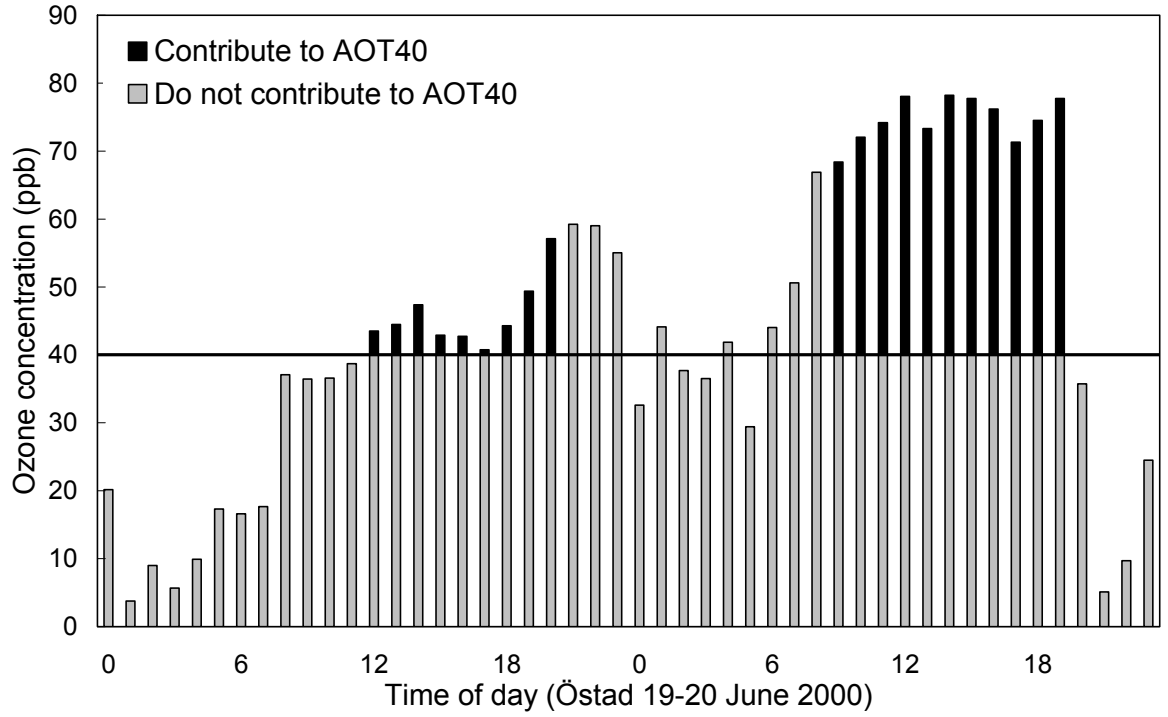

Figure A1. Calculation of AOT40 (O_3 concentrations accumulated over a threshold concentration of 40 ppb) during hours 8 to 20 for Östad 19–20 June 2000.

Gaussian method to estimate the AOT-index

In the Gaussian method it was assumed that the hourly O_3 concentration (C) has a Gaussian probability density function ($f(C)$) with a mean μ and standard deviation σ. AOT values with different threshold concentrations (c_0) can be calculated based on time-integrated O_3 concentration from a passive diffusion sampler (μ) in combination with an estimate of the O_3 standard deviation (σ):

$$AOT_{c_0} = t\int_{c_0}^{\infty}(C - c_0)f(C)dc \qquad \text{(Eq. 2)}$$

The variable t is the duration of the monitoring period in hours. The derivation of the expanded formulae directly applicable for numerical determination of AOTX is:

$$AOT_{c_0} = t\left[\sigma\varphi\left(\frac{\mu - c_0}{\sigma}\right) + (\mu - c_0)\Phi\left(\frac{\mu - c_0}{\sigma}\right)\right] \qquad \text{(Eq. 3a)}$$

where

$$\varphi(x) = \frac{1}{\sqrt{2\pi}}e^{-x^2/2} \qquad \text{(Eq. 3b)}$$

i.e. the standard Gaussian distribution having $\mu = 0$ and $\sigma = 1$. $\Phi(x)$ is the corresponding cumulative density function.

24-hour AOT values are given from Equation 2 and 3. 12-hour daytime AOT values are more relevant in risk assessment of O_3 damage on vegetation. It can be calculated from 24-hour AOT by the use of a conversion factor (α, Equation 4).

$$AOT_{24h} = \alpha \times AOT_{12h} \qquad \text{(Eq. 4)}$$

Trigonometric method to estimate the AOT-index

In the trigonometric method the diurnal O_3 concentration is represented by a sine function with amplitude A that is half the diurnal O_3 concentration range and a frequency of 1 day^{-1}, oscillating around the average O_3 concentration. AOT values with different thresholds (c_0) are calculated for one average day and then multiplied by the number of days the monitoring was in progress (D).

$$AOT_{c_0} = D \times \int_{h_1}^{h_2}(g(h) - c_0)dh \qquad \text{(Eq. 5a)}$$

where

$$g(h) = \mu + A \times \sin\left(\frac{2\pi(h - h_0)}{24}\right) \qquad \text{(Eq. 5b)}$$

Equation 5 can be expanded and simplified into Equation 6.

$$AOT_{c_0} = D\left((\mu - c_0)(h_2 - h_1) + \frac{12A}{\pi}\left(\cos\left(\frac{\pi(h_1 - h_0)}{12}\right) - \cos\left(\frac{\pi(h_2 - h_0)}{12}\right)\right)\right) \qquad \text{(Eq. 6a)}$$

where

$$h_1 = h_0 + \frac{12}{\pi}\sin^{-1}\left(\frac{c_0 - \mu}{A}\right) \quad \text{(Eq. 6b)}$$

and

$$h_2 = 2h_0 + 12 - h_1 \quad \text{(Eq. 6c)}$$

In Equation 6, h is the time in hours since midnight and h_0 is a phase displacement which synchronises the sine function with the O_3 concentration diurnal variation with an afternoon maximum and night-time minimum. For example, if h_0 is set to 12, $g(h)$ will reach its minimum at 6:00 in the morning (h=6) and its maximum at 18:00 in the afternoon. The integration limits h_1 and h_2 are the values of h when the modelled O_3 concentration intercepts with the threshold value ($g(h)=c_0$). For calculation of 12-hour AOT (8:00–20:00) values of $h_1<8$ are set to 8 and values of $h_2>20$ are set to 20.

2. The flux-based O_3 index POD_Y

The phytotoxic O_3 dose (POD_Y) is expressed as the accumulated stomatal flux of O_3 per unit projected sunlit leaf area (PLA) above a flux threshold of Y nmol m^{-2} PLA s^{-1} (unit: mmol m^{-2} PLA). In this thesis the stomatal flux of O_3 is modelled according to the methodology described in the UNECE CLRTAP Mapping Manual (LRTAP Convention, 2004). The stomatal O_3 flux model has been parameterised for a limited number of crop and tree species. In addition, a simplified flux-based method has been developed, recommended to indicate the risk for O_3 damage to a generic crop and a generic deciduous tree in large-scale modelling (LRTAP Convention, 2004; Simpson and Emberson, 2006). Parameterisation of the stomatal flux algorithms for the species used in this thesis can be found in Table A1. A lower threshold is used for the generic crop than recommended for specific crops, making the method numerically more robust (Tuovinen et al., 2007).

POD_Y is accumulated over a period of time corresponding to the part of the growing season when the plant is considered to be sensitive to O_3. Only hours when the stomatal flux of O_3 (F_{st}) exceeds a threshold (Y nmol m^{-2} s^{-1}) contributes to POD_Y.

$$POD_Y = \int \max(F_{st} - Y, 0)\,dt \quad \text{(Eq. 7)}$$

The resistance analogue

A resistance analogue is used to calculate the stomatal flux of O_3 (F_{st}). The O_3 molecule must overcome a series of resistances to gaseous flux on its way from the air above the canopy into the leaf (Figure A2). First, the O_3 molecule must pass from the air stream overhead down to the leaf (aerodynamic resistance). The aerodynamic resistance is determined by e.g. the wind speed and the roughness of the surface. Next the O_3 molecule must cross a thin layer of stagnant air at the leaf surface (leaf boundary layer resistance). The leaf boundary layer resistance is determined by e.g. wind speed and leaf dimensions. Thereafter the O_3 molecule can either enter the leaf through the stomatal apertures (stomatal resistance) or deposit on the leaf surface (resistance to leaf surface deposition).

In the F_{st} calculation, the O_3 concentration at the top of the canopy ($C(z)$) is assumed to be a reasonable estimate of the concentration at the surface of the laminar leaf boundary layer near the sunlit upper canopy leaves. Then F_{st} is given by:

$$F_{st} = C(z) \times \frac{1}{r_b + r_c} \times \frac{g_s}{g_s + g_{ext}} \quad \text{(Eq. 8)}$$

where g_s is the stomatal conductance (r_s^{-1}, mmol O_3 m^{-2} PLA s^{-1}). The $1/(r_b+r_c)$ term is the deposition rate to the leaf determined by the leaf boundary layer resistance (r_b) and the leaf surface resistance (r_c). $g_s/(g_s+g_{ext})$ represent the fraction of O_3 taken up through the stomata, where $1/g_{ext}$ is the external leaf resistance. r_c is given by $1/(g_s + g_{ext})$ and r_b is estimated from the cross-wind leaf dimension (L) and the wind speed at height z ($u(z)$):

$$r_b = 1.3 \times 150 \times \sqrt{\frac{L}{u(z)}} \quad \text{(Eq. 9)}$$

The core of the stomatal O_3 flux model is the stomatal conductance multiplicative algorithm, which is presented in Jarvis (1976) and further developed specifically to model O_3 uptake to plants (Emberson et al. 2000a,b). It includes functions accounting for the limiting effects of various abiotic factors on g_s, thereby regulating the O_3 flux into the plant leaf:

$$g_s = g_{max} \times \left[\min\left(f_{phen}, f_{O_3}\right)\right] \times f_{light} \times \max\left\{f_{min}, \left(f_{temp} \times f_{VPD} \times f_{SWP}\right)\right\} \quad \text{(Eq. 10)}$$

where g_{max} is the species-specific maximum g_s. The functions f_{phen}, f_{O3}, f_{light}, f_{temp}, f_{VPD} and f_{SWP} are expressed in relative terms (take values between 0 and 1) as a proportion of g_{max}. These parameters allow for the influence of phenology, O_3 and the environmental variables (irradiance, temperature, water vapour pressure deficit (VPD) and soil water potential (SWP)) on g_s to be estimated.

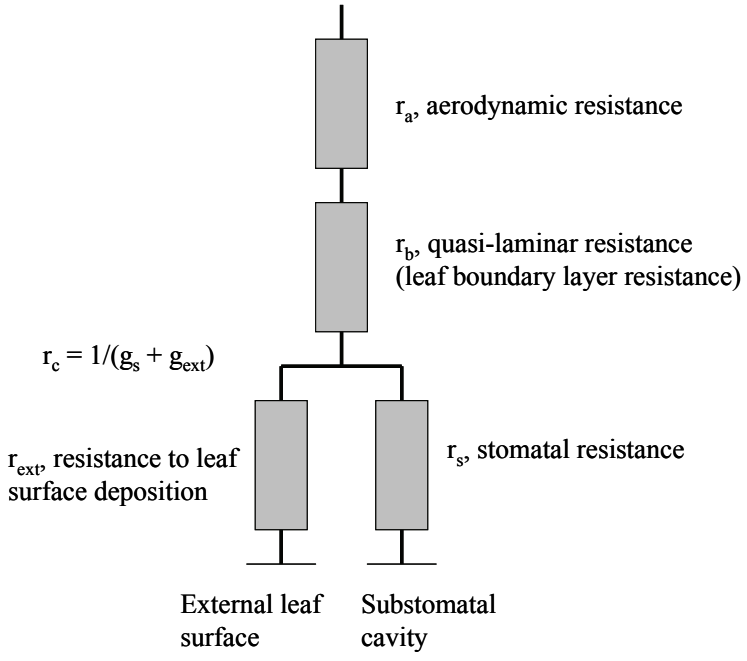

Figure A2. The resistance analogue on which the stomatal O_3 flux calculations are based.

Phenology and ozone

The phenology function (Figure A3) for crops can be based on a fixed time interval or effective temperature sum accumulation. The effective temperature sum accumulation takes into account the temperature dependence of growth and is generally accepted to describe plant development more accurately. However, in **Paper V** it was decided to use a fixed time interval to guarantee that the same period of time was used when comparing measurements and model output. The start (A_{start}) and end (A_{end}) of the accumulation period for wheat was calculated using a latitude model to estimate mid-anthesis. For potato, A_{start} was estimated using local information on sowing date. For a generic crop (**Paper VI**) a three month time-window for stomatal O_3 flux accumulation (with f_{phen} =1) is used to bypass the uncertainty in the timing of the relevant time-interval, which, especially for crops, is rather short. The time interval is centred around mid-anthesis, which is estimated using the latitude model. The start (SGS) and end (EGS) of the generic deciduous tree stomatal O_3 accumulation period (**Paper VI**) is based on latitude and altitude.

Mid-anthesis = (2.57 * latitude) + 40
SGS = 105 + (latitude - 50) * 1.5 + (altitude/1000) * 10
EGS = 297 - (latitude - 50) * 2 - (altitude/1000) * 10

f_{phen} if $A_{start} \leq yd < (A_{start} + f_{phen\_c})$
$= (1\text{-}f_{phen\_a}) * ((yd - A_{start})/f_{phen\_c}) + f_{phen\_a}$
if $(A_{start} + f_{phen\_c}) \leq yd \leq (A_{end} - f_{phen\_d})$
$= 1$
if $(A_{end} - f_{phen\_d}) < yd \leq A_{end}$
$= (1 - f_{phen\_b}) * ((A_{end} - yd)/f_{phen\_d}) + f_{phen\_b}$

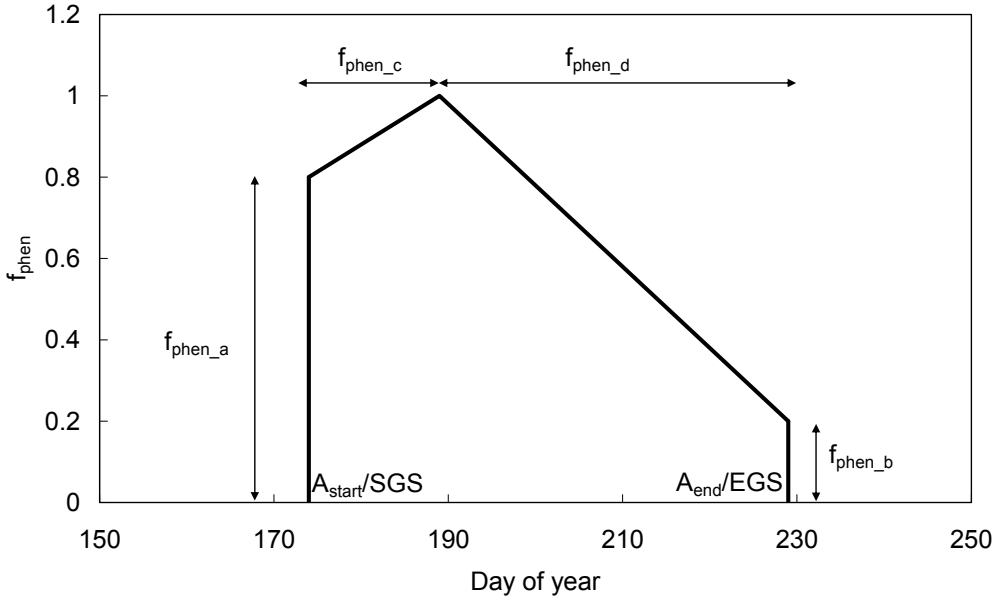

Figure A3. The f_{phen} function, here exemplified with wheat at the latitude where Östad is situated.

The part of Equation 10 related to f_{phen} and f_{O3} is a most limiting factor approach; i.e. g_s is limited by either senescence due to normal aging or premature senescence induced by O_3. The f_{O3} function only comes into operation if it has a stronger senescence-promoting effect than

normal senescence. The f_{O3} function is assumed to never limit the stomatal conductance for the generic crop and generic deciduous tree (i.e. f_{O3}=1).

f_{O3} $= (1 + (AOT0/40)^{5})^{-1}$ (potato)
$= (1 + (POD_0/11.5)^{10})^{-1}$ (wheat)
$= (1 + (POD_0/14)^{8})^{-1}$ in the 2010 update of the Mapping Manual

Light

The f_{light} function is approximately an on-off function. The stomatal conductance increases rapidly as light levels increase and saturates to a large extent already at low light levels in the morning.

$f_{light} = 1 – EXP((-light_a) * PPFD$

Temperature

The f_{temp} function is a bell-shaped optimum curve. The stomatal conductance gradually increases as temperature increases, reaching a maximum and then gradually declines as temperature increases beyond the optimum.

f_{temp} if $T_{min} < T < T_{max}$
$= \max (f_{min}, [(T - T_{min})/(T_{opt} - T_{min})] * [(T_{max} - T)/(T_{max} - T_{opt})]^{bt})$
$bt = (T_{max} – T_{opt})/(T_{opt} – T_{min})$
if $T_{min} > T > T_{max}$
$= f_{min}$

Air and soil humidity

High VPD levels result in stomatal closure to reduce the high rate of water transpiring out of the leaf under such conditions. The f_{VPD} function reduces stomatal conductance linearly between a non-limiting plateau and a strongly limiting plateau.

$f_{VPD} = \min (1, \max[f_{min}, ((1-f_{min}) * (VPD_{min} – VPD)/(VPD_{min} – VPD_{max})) + f_{min}])$

Air temperature is typically decreasing in the afternoon, which is normally followed by declining VPD. However, if the plant has experienced substantial water loss during the day, re-opening of the stomata in the afternoon does generally not occur. This is taken into account in the model by calculating the VPD sum (ΣVPD, the sum of hourly VPD values since dawn). If the ΣVPD exceeds a critical value, then stomatal re-opening in the afternoon does not occur. The ΣVPD routine is not yet included for forest trees.

if $\Sigma VPD \geq \Sigma VPD_{crit}$
$g_{s\_hour\_n+1} \leq g_{s\_hour\_n}$

The f_{SWP} function is similar to the f_{VPD} function. Dry soil results in stomatal closure to reduce water loss. The f_{SWP} function is assumed to never limit the stomatal conductance for the generic crop and generic deciduous tree (i.e. f_{SWP}=1).

$f_{SWP} = \min (1, \max [f_{min}, ((1-f_{min}) * SWP_{min} – SWP)/(SWP_{min} – SWP_{max})) + f_{min}])$

Table A1. Parameterisation of the stomatal flux algorithms for wheat and potato (**Paper V**), a generic crop (**Paper III, VI**) and a generic deciduous tree (**Paper VI**) according to UNECE CLRTAP Mapping Manual (LRTAP Convention, 2004).

Parameter	**Unit**	**Wheat**	**Potato**	**Generic crop**	**Generic deciduous tree**
Y	nmol O_3 m^{-2} PLA s^{-1}	6	6	3	1.6 (1)*
g_{max}	mmol O_3 m^{-2} PLA s^{-1}	450 (500)*	750	450 (500)*	150
f_{min}	(fraction)	0.01	0.01	0.01	0.1
A_{start}/SGS	yearday	174	156	Latitude model	Latitude model
A_{end}/EGS	yearday	229	226	Latitude model	Latitude model
f_{phen_a}	(fraction)	0.8 (0.7)*	0.4		0
f_{phen_b}	(fraction)	0.2 (0.3)*	0.2		0
f_{phen_c}	days	15	20		15
f_{phen_d}	days	40	50		20
$light_a$	constant	0.0105	0.005	0.0105	0.006
T_{min}	°C	12	13	12	0
T_{opt}	°C	26	28	26	21
T_{max}	°C	40	39	40	35
VPD_{max}	kPa	1.2	2.1	1.2	1
VPD_{min}	kPa	3.2	3.5	3.2	3.25
ΣVPD_{crit}	kPa	8	10	8	
g_{ext}	m s^{-1}	1/2500	1/2500	1/2500	1/2500
Leaf dimension	m	0.02	0.04	0.02	0.07

* values in brackets represent the revised parameterisation from the 2010 update of the Mapping Manual

References

Emberson, L., Simpson, D., Tuovinen, J. P., Ashmore, M. and Cambridge, H. M. 2000a. Towards a model of ozone deposition and stomatal uptake over Europe. EMEP MSC-W Note 6/2000. Norwegian Meteorological Institute, Oslo, Norway. Available at www.emep.int.

Emberson, L. D., Ashmore, M. R., Cambridge, H. M., Simpson, D. and Tuovinen, J. P. 2000b. Modelling stomatal ozone flux across Europe. *Environmental Pollution* **109**, 403-413.

Jarvis, P. G. 1976. The interpretation of the variations in leaf water potential and stomatal conductance found in canopies in the field. *Philosophical Transactions of the Royal Society, London B* **87**, 593-610.

LRTAP Convention 2004 (updated 2010*)*. Manual on methodologies and criteria for Modelling and Mapping Critical Loads & Levels and Air Pollution Effects, Risks and Trends. Available and continuously updated at www.icpmapping.org.

Simpson, D. and Emberson, L. 2006. Ozone fluxes - updates, chapter 5 in EMEP status report 1/2006, Transboundary acidification, eutrophication and ground level ozone in Europe since 1990 to 2004. Available at www.emep.int.

Tuovinen, J. P., Simpson, D., Emberson, L., Ashmore, M. and Gerosa, G. 2007. Robustness of modelled ozone exposures and doses. *Environmental Pollution* **146**, 578-586.

ISBN 978-91-85529-47-6